Radiat Environ Biophys (1998) 37: 293–310

ORIGINAL PAPER

W. Rühm · A. M. Kellerer · G. Korschinek
T. Faestermann · K. Knie · G. Rugel · K. Kato
E. Nolte

The dosimetry system DS86 and the neutron discrepancy in Hiroshima – historical review, present status, and future options

Received: 7 May 1998 / Accepted in revised form: 16 September 1998

Abstract The historical development of the dosimetry systems for Hiroshima and Nagasaki is outlined from the time immediately after the A-bomb explosions to the publication of the dosimetry system DS86 in 1987, and the present status of the so-called Hiroshima neutron discrepancy is summarized. Several long-lived radionuclides are discussed with regard to their production by neutrons from the A-bomb explosions. With the exception of ^{63}Ni, these radionuclides have not, up to now, been measured in samples from Hiroshima and Nagasaki. Two of them, ^{63}Ni in copper samples and ^{39}Ar in granite samples, were predominantly produced by fast neutrons. ^{63}Ni can be determined by accelerator mass spectrometry with a gas-filled analyzing magnet. It should be measurable, in the near future, in copper samples up to 1500 m from the hypocenter in Hiroshima. ^{39}Ar can be measured in terms of low-level beta-counting. This should be feasible up to a distance of about 1000 m from the hypocenter. Three radionuclides, ^{10}Be, ^{14}C , and ^{59}Ni, were produced predominantly by thermal neutrons with smaller fractions due to the epithermal and fast neutrons, which contribute increasingly more at larger distances from the hypocenter. State-of-the-art accelerator mass spectrometry is likely to permit the determination of ^{10}Be close to the hypocenter and of ^{14}C up to a distance of about 1000 m. ^{59}Ni should be detectable up to a distance of about 1000 m in terms of accelerator mass spectrometry with a gas-filled magnet. The measurements of ^{10}Be, ^{14}C, ^{39}Ar, ^{59}Ni – and potentially of ^{131}Xe – can be performed in the same granitic sample that was already analyzed for ^{36}Cl, ^{41}Ca, ^{60}Co, ^{152}Eu, and ^{154}Eu. This will provide extensive information on the neutron spectrum at the specified location, and similarly complete analyses can conceivably be performed on granite samples at other locations.

W. Rühm (✉) · A. M. Kellerer · K. Knie · G. Rugel
Radiobiological Institute, University of Munich,
Schillerstrasse 42, D-80336 Munich, Germany

G. Korschinek · T. Faestermann · E. Nolte
Faculty of Physics, Technical University of Munich,
D-85747 Garching, Germany

K. Kato
Suzugamine Women's College,
Inokuti, Nishi-ku, 733-8623 Hiroshima, Japan

Introduction

The follow-up of the A-bomb survivors in Hiroshima and Nagasaki has become the major source of information on the late effects of radiation exposures. While the excess cancer rates are especially pronounced among the few thousand survivors who were exposed to high, life-threatening doses, there is also substantial evidence concerning the effects among the large majority of survivors who were exposed to moderate or low doses. This has made it possible to derive risk estimates for small radiation exposures, as required for radiation protection purposes. The analysis depends equally on the information of health effects and on the determination of the gamma-ray and neutron doses received by each individual in the cohort. It has often been assumed that the contribution of neutrons to the observed health effects is minor. However, this is an unproven assumption, especially at low doses where, according to various radiobiological observations, neutrons can be far more effective than gamma-rays. There is, accordingly, considerable interest in the resolution of apparent inconsistencies in the neutron dosimetry for the A-bomb survivors.

The current dosimetry system, DS86, was developed in a large international effort, but even when it was first released, it was stated that – in view of unresolved divergencies between measurements and computations – the neutron doses in Hiroshima and Nagasaki need to be considered as tentative [1]. Since that time, evidence has accumulated that appears to support the neutron dose estimates in Nagasaki, while it indicates that in Hiroshima, DS86 may have substantially underestimated the neutron doses at distances beyond 1000 m from the hypocenter.

The first indications of inconsistencies – during the develoment of DS86 and subsequent to its release – were seen when measurements of ^{60}Co, ^{152}Eu, and ^{154}Eu were com-

pared to the DS86 predictions. These radionuclides, with their respective half-lives of 5.27, 13.33, and 8.8 years, were determined by gamma-spectrometry measurements. Their half-lives are sufficiently long to assure that, several decades after the explosions, a sufficient fraction of the initial activity still remains. On the other hand, they are sufficiently short to ensure reasonably high activities. Nowadays, that is, more than 50 years after the explosions, it is becoming increasingly difficult to detect such radionuclides.

Recently, new analytical capabilities in terms of accelerator mass spectrometry (AMS) have become available; they permit the detection of long-lived radionuclides produced by neutrons from the A-bomb explosions. With this technique, minute amounts of nuclides with specified mass A can be measured directly. Consequently, one is not constrained by low counting rates due to long half-lives. The disadvantage of conventional mass spectrometry is that it is difficult to distinguish between isobars or molecules with the same mass. The use of an accelerator and of specific detection methods developed in nuclear physics for ions with energies of several MeV per nucleon removes this disadvantage; the undesired molecules and isobars can be separated out. This technique has already been used to determine ^{36}Cl and ^{41}Ca – with half-lives of $3 \cdot 10^5$ and 10^5 years, respectively – in samples from Hiroshima and Nagasaki; a number of other radionuclides are of interest for future studies.

Several authors (e.g., [2, 3]) have contributed excellent historical reviews to the dosimetric reassessment that led to the current dosimetry system DS86 [1]. The development of the dosimetry systems for Hiroshima and Nagasaki is here briefly outlined again and related to work performed after the release of DS86. Reference is made throughout in terms of free-in-air kerma. There will be no consideration of shielding problems and their unresolved issues such as the problem of the the 'factory workers' in Nagasaki. Recent efforts to measure long-lived radioisotopes are then described, and additional long-lived radioisotopes are assessed that could serve as neutron monitors for Hiroshima.

If not otherwise stated, all data on half-lives, isotopic abundancies, and thermal cross-sections are taken from Pfennig et al. [4]. Q-values are taken from Firestone [5]. Sample locations or locations with specified dose are given in terms of ground ranges or, if more appropriate, in terms of slant ranges. Ground range denotes the distance between the location of interest and the hypocenter of the explosion, the hypocenter being the vertical projection of the actual location of the explosion, i.e., the epicenter, onto the ground. Slant range denotes the actual distance of the location of interest to the epicenter.

The evolution of the dosimetry systems

Early activities

The investigation of the effects of the atomic bomb explosion started when Prof. Yoshio Nishina entered Hiroshima on behalf of the Japanese government, 1 day after the explosion. Nishina was a well-known quantum physicist who had studied in the laboratory of Niels Bohr in Denmark before the war and was familiar with nuclear physics. The degree of the damage, effects such as molten surfaces of roof tiles, and measurable radioactivity on the ground near the hypocenter led him to the immediate conclusion that only a nuclear-type weapon could have caused such effects.

During the subsequent weeks, several Japanese research groups started to work in Hiroshima and Nagasaki. Early activities concentrated, for example, on the identification of the hypocenters of both explosions. By geometrically analysing thermal-radiation shadows of objects Kimura and Tajima [6] derived an accurate estimate for the burst heights of Hiroshima (577 ± 20) m and Nagasaki (490 ± 25) m. Uda et al. [7] recorded meteorogical data for August 6 for Hiroshima and August 9 for Nagasaki. They used data from records from the former Hiroshima District Meteorological Observatory, located 3.6 km from the hypocenter, and the former Nagasaki Meteorological Station, located 4.5 km from the Nagasaki hypocenter [7]. Later, these data proved to be useful for transport calculations that simulated the propagation of neutrons and gamma-rays from the epicenter to the ground.

Radioactivity measurements covered large areas within both cities. Regions with higher radioactivity levels due to fallout, washed out from the atmosphere by the 'black rain', were identified at a distance of about 3 km to the west in Hiroshima and at similar distance to the east in Nagasaki (see e.g., [8–13]). In addition, a number of short-lived radionuclides were measured, such as ^{56}Mn ($T_{1/2}$ = 258 h), ^{24}Na ($T_{1/2}$ = 14.96 h), and ^{46}Sc ($T_{1/2}$ = 83.82 days), that were produced by low-energy neutron activation of soil and other materials close to the hypocenters. Their activities were determined according to the distance from the hypocenter and time (see e.g., [13–15]). It is of particular interest that one radionuclide, ^{32}P – a pure beta-emitter with half-life of 14.26 days – was produced exclusively by fast neutrons through the reaction ^{32}S(n,p)^{32}P. The Q value of this reaction is –0.9 MeV, and its cross-section begins to be appreciable at a neutron energy of about 2 MeV. On August 13 and 14, samples of electric power poles were collected which contained sulfur used as an adhesive for insulators. On August 15, ^{32}P was measured for the first time at Kyoto University in three samples using a Geiger Mueller counter. In order to identify ^{32}P unambigously, half-life and beta-ray energy were also determined [16]. On September 20, Yamasaki and Sugimoto also measured, as a function of distance from the hypocenter, the ^{32}P in similar samples [17, 18]. These data represent, up to now, the only measurement of a radionuclide produced by fast neutrons in Hiroshima.

Starting in late 1946, these first activities were coordinated by the Atomic Bomb Casuality Commission (ABCC), which later became the Radiation Effects Research Foundation (RERF). More detailed descriptions of the early studies and their circumstances are given elsewhere [2, 19–21].

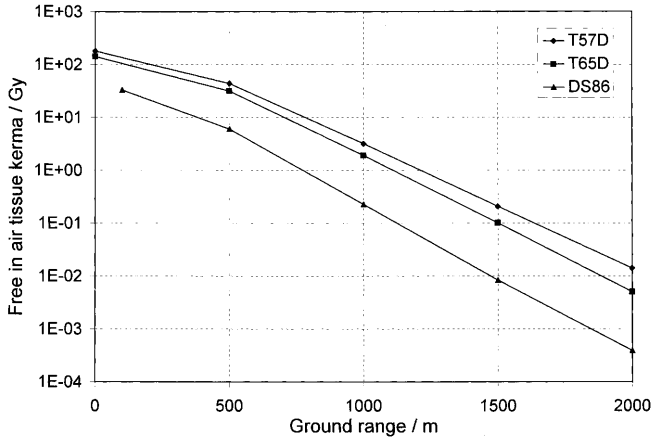

Fig. 1 Free-in-air neutron kerma in Hiroshima according to T57D [27], T65D [28], and DS86 [1]. *Lines between symbols* serve as eye guide

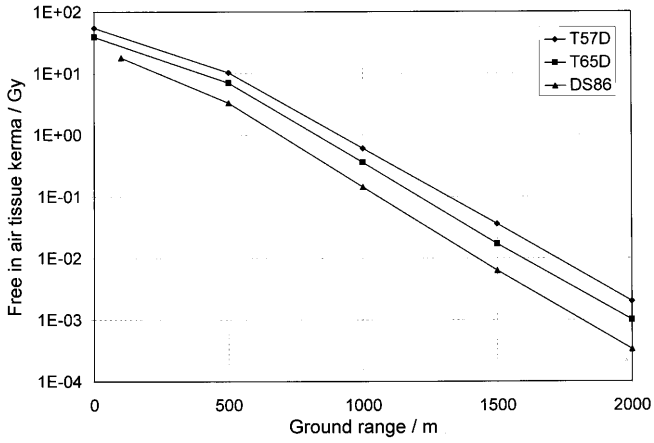

Fig. 3 Free-in-air neutron kerma in Nagasaki according to T57D [27], T65D [28], and DS86 [1]. *Lines between symbols* serve as eye guide

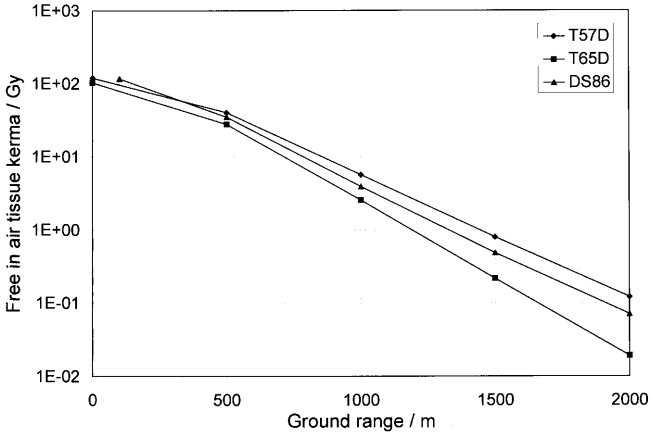

Fig. 2 Free-in-air gamma-ray kerma in Hiroshima according to T57D [27], T65D [28], and DS86 [1]. *Lines between symbols* serve as eye guide

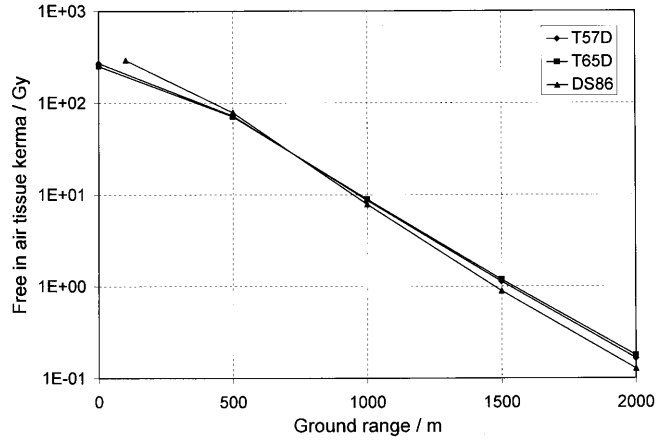

Fig. 4 Free-in-air gamma-ray kerma in Nagasaki according to T57D [27], T65D [28], and DS86 [1]. *Lines between symbols* serve as eye guide

Tentative 1957 dosimetry (T57D)

In the late 1940s and early 1950s, first reports appeared regarding cataracts [22, 23] and leukemia [24, 25] among A-bomb survivors. The findings indicated the need for reliable estimates of individual radiation doses to the survivors. An attempt was then made to estimate, as a function of distance from the hypocenters in Hiroshima and Nagasaki, an air dose, which was, in essence, the quantity later termed free-in-air tissue kerma (Figs. 1–4). While the analysis was based on nuclear test explosions at the Nevada test site (NTS), it must be noted that, in contrast to the Nagasaki-type bomb, a device similar to the Hiroshima bomb has never been tested. The dosimetry for Hiroshima was, thus, based only on calculations [26]. For shielding studies, two typical Japanese houses were built on the NTS, and the shielding factors for neutron and gamma-radiation were quantified in terms of a simple parameter, the so-called house-penetration distance (which was defined as the distance along the ray path from the first point of entry into the house to the location of interest). For about 14 000 survivors, typical shielding histories were derived from interviews, and their distances to the hypocenter and house-penetration distances were determined. With this information, the so-called Tentative 1957 Dosimetry was established [27].

Tentative 1965 doses (T65D)

In subsequent years, the T57D was supplanted by new information from further test explosions and from the operation BREN (Bare Reactor Experiment Nevada). In this experiment, a nuclear reactor and a ^{60}Co-source were mounted on a tower, 465 m in height, an approach that became necessary when the weapons moratorium went into effect in 1958. For Hiroshima, the results of test explosions and of operation BREN were combined with insights from reactor experiments [2]. As a result of these efforts, the estimated yield of the Hiroshima bomb changed from 18.5 kt

to 12.5 kt. Neutron air doses were, by a factor of up to 2.6, smaller than their values in T57D for both cities (Figs. 1 and 3). Gamma air doses did not change for Nagasaki, but decreased significantly for Hiroshima (Figs. 2 and 4). This was partly due to the fact that, because of assumed differences in the gamma-ray source terms, the new relaxation length for gamma-rays was smaller for Hiroshima than for Nagasaki [26, 28].

Other major advances were made in evaluating the effects of shielding by terrain and adjacent structures, and a more sophisticated procedure was developed for estimating the individual transmission factors that had to be applied to the air dose for persons who were exposed in typical Japanese houses. By August 1967, dose estimates were given for a total of 84 000 survivors, including more than 28 000 cases where shielding histories were complete [28].

In parallel to the development of T65D at the Oak Ridge National Laboratory, results became available of thermoluminescence dosimetry on roof tiles performed for both cities by the Kyoto University and the Japanese National Institute for Radiological Sciences. For Nagasaki, these data were in agreement with T57D and T65D gamma-ray doses. For Hiroshima, these data were in better agreement with the new T65D gamma-ray doses than with T57D [29–31].

To estimate neutron doses, measurements were performed – at different distances from the hypocenters – of the ^{60}Co which had been produced in reinforcing steel bars of ferro-concrete buildings by thermal neutrons via the reaction $^{59}\mathrm{Co}(n,\gamma)^{60}\mathrm{Co}$ [31–33]. For Hiroshima, the results were about 20% below the T65D estimates, which was within the stated estimates for the range of errors. For Nagasaki, however, the two measurements on samples 590 m and 1030 m from the hypocenter were 17% and 42% above the T65D neutron dose estimates. This discrepancy for Nagasaki was noted but seemed unimportant, since the neutron dose was a small fraction of the total dose in Nagasaki; as will be pointed out subsequently, however, this discrepancy has not been confirmed by more recent measurements of ^{36}Cl.

In view of the overall consistency of calculations and measurements, T65D was judged, during the 1970s, to be reliable. Things changed considerably when an article by Rossi and Mays appeared in 1978 [34]. These authors used T65D total free in air tissue kermas and corrected for body absorption to calculate marrow doses for the survivors of Hiroshima and Nagasaki. In this way, they showed that for the same total absorbed dose in the marrow, the number of leukemias per million person-years was larger for Hiroshima than for Nagasaki. Rossi and Mays attributed this larger leukemia incidence in Hiroshima to the larger neutron component in this city compared with Nagasaki, and estimated an increasing relative biological effectiveness (RBE) of neutrons at decreasing neutron absorbed dose, reaching a value of about 60 at a neutron dose of 1 rad (10 mGy). This was in agreement with earlier estimates published by Rossi and Kellerer [35]. With regard to radiation protection practice, the authors advised that 'the doses received from fast neutrons be kept at about one order of magnitude below currently accepted permissible limits' [34]. The results caused considerable concern among the scientific community [36, 37], and several groups began to reevaluate the T65D estimates.

Already in the early 1980s, preliminary calculations by Loewe and Mendelsohn [38] suggested that the T65D doses did, indeed, require substantial revision. Using their tentative results and the methodology of Rossi and Mays [34], Loewe and Mendelsohn were then able to show that the differences in the leukemia incidence in Hiroshima and Nagasaki disappeared [38].

Dosimetry system 1986 (DS86)

By 1986, a full revision of the T65D doses was produced as the fruit of an extensive international co-operation [1]. The first basis of the Dosimetry System 1986 (DS86) involved calculations of the neutron and gamma-ray source terms of both explosions in terms of complex algorithms that simulated the transport of neutrons and gamma-rays in hot moving material. The second stage was composed of extensive computer calculations which simulated the entire neutron and gamma-ray transport from the epicenter to the organ of interest, including transport through air, backscattering by the ground, and shielding by surrounding structures and the human body.

All available data (pressure versus time measurements, blast wave damage, charring of cypress wood, thermoluminescence measurements, neutron activation measurements of ^{32}P, etc.) were scrutinized again, and a best yield estimate of 15 ± 3 kt for Hiroshima and 21 ± 2 kt for Nagasaki was made [39]. With regard to neutrons, it must be noted that the computed source terms could not be compared directly to experimental data. However, the so-called Little Boy Replica reactor (which consisted of the casing of the Hiroshima bomb containing a uranium mass just sufficient to be at delayed criticality), for example, permitted measurements of sulfur activation that indicated reasonable agreement between calculations and measurements [40].

Neutron and gamma-ray transport through air was calculated in terms of discrete ordinate transport techniques. Free-in-air kerma for neutrons and gamma-rays 1 m above ground was given as a function of distance from the hypocenter for prompt and for delayed radiation. These calculations included height of the explosions, bomb yields, meteorological data for the days of the bombing, information on the typical chemical composition of the ground for both cities, etc. [41].

For Nagasaki, the neutron kerma was – primarily due to the assumed air humidity of 80% – lower than the T65D values by a factor of as much as 3 for larger distances (Fig. 3). The T65D dosimetry had been based on data obtained under very dry conditions at the NTS, and no modifications had been made to account for air humidity. Gamma-ray kerma is not substantially affected by air humidity, and accordingly, no major revision has occured since T57D for Nagasaki (Fig. 4).

For Hiroshima, the most notable change was the reduction of the neutron kermas by up to about one order of magnitude at larger distances (Fig. 1). Apart from the effect of air humidity, this was due to the fact that an energy spectrum was calculated for the Hiroshima explosion that differed substantially from the source terms assumed in T65D. Gamma-ray kermas for DS86 were larger than for T65D by a factor ranging from 2 at close distances to almost 4 at larger ground ranges (Fig. 2). 'No attempt was made … to retrace the T65D work to see where the difference arose' [42]. The critical point may have been that experimental data from test explosions with Nagasaki-type bombs at the NTS and from mock-up experiments had to be modified in a variety of ways to estimate T65D gamma-ray kerma for Hiroshima.

In order to quantify house and terrain shielding, models of Japanese houses and Japanese house clusters with typical dimensions and materials were developed. Neutron and gamma-ray spectra resulting from adjoint Monte Carlo transport calculations were coupled to the free-in-air fluences, and energy and angular distributions of neutrons and gamma-rays at specified locations inside or adjacent to a house cluster were calculated. This technique was validated by its application to houses and house clusters that were used in the BREN experiments. Compared to T65D shielding, gamma-ray transmission factors (defined as the ratio of the gamma-ray kerma inside the house to free in air gamma-ray kerma) were reduced by a factor of about 2. This was due to the fact that DS86 neutron spectra were different from the neutron spectra used in the NTS experiments, which correspondingly changed production of secondary gamma-rays by interaction of neutrons with wall material.

The gamma-ray estimates were judged to be reliable for several reasons when DS86 was released. As stated, Loewe and Mendelsohn [38] had already pointed out, in the early 1980s, that the revised dose estimates removed the discrepancies reported by Rossi and Mays [34]. In addition, new thermoluminescence measurements for ground ranges greater than 1000 m were in better agreement with the DS86 gamma-ray kerma values than with the T65D estimates. Nevertheless, for Nagasaki a small deviation was seen for about 1400 m ground range, the thermoluminescence measurements being about 10% too low. Furthermore, for Hiroshima, '…measurements of all of the laboratories differed significantly from calculated values at distances beyond 1000 m' [43]. For example, thermoluminescence measurements exceeded the DS86 calculations by about 30% at a distance of about 1400 m from the hypocenter. It was concluded that '…additional comparative measurements beyond 1000 m in Hiroshima are called for' [43].

For neutrons, additional neutron activation data had become available after the release of T65D. ^{152}Eu, predominantly produced by thermal neutrons, was measured by use of high resolution in situ gamma-ray spectrometry [44, 45]. The results showed no significant discrepancies from the DS86 calculations. However, for ground distances beyond 1000 m, the uncertainties precluded conclusions on the validity of the DS86 neutron fluences. Significant discrepancies became evident, however, between the ^{60}Co activation data from Hashizume et al. [31] and the DS86 calculations. The measured ^{60}Co activities were about 50% below DS86 predictions for a ground range of about 200 m in Hiroshima, but were about a factor of 3 times greater for ground ranges of 1000 m in Nagasaki and for 1200 m in Hiroshima [46]. Therefore, in the final report of DS86, it was stated that '…the conclusion of this chapter on neutron measurements must be that the neutron doses are in doubt until further work is done' [47].

Figures 1–4 give, as a function of ground range, the neutron and gamma-ray free-in-air tissue kermas that were estimated in T57D, T65D, and DS86 for Nagasaki and Hiroshima.

Developments after the release of DS86

After the release of DS86, efforts were continued to validate the radiation transport calculations and to enlarge the existing experimental database.

From the results of DS86, it appeared that the calculated thermal neutron activation was seriously in error both for Hiroshima and Nagasaki. It is important to realize at this point that due to limited computer power at the time, most of the transport calculations in DS86 were performed in terms of a limited number of energy groups [46]. For example, thermal neutrons were described by a single energy group ranging from 10^{-5} to 0.4 eV. Accordingly, the calculations were subsequently repeated with cross-section sets for a larger number of energy groups. Kaul et al. [48] found, thus, about 50% less activation close to the hypocenter in Nagasaki when they used 174 neutron energy groups. Furthermore, computations were performed with transport codes different from those that were employed in DS86. For example, Rühm et al. [49] used the Monte Carlo code MORSE with 118 energy groups for the entire range from 10^{-5} eV to 14.9 MeV, and 19 groups between 10^{-5} and 0.4 eV. In contrast to the results of Kaul et al., they found about 50% more thermal activation close to the hypocenter in Hiroshima than DS86 predicted. In addition, benchmark tests were carried out with MCNP, another Monte Carlo code which allows the use of continuous cross-section sets, to explore its applicability to deep penetration problems. It was shown that this code produces reasonable results for moderators containing hydrogen, carbon, nitrogen, and oxygen as the main components, for moderator thicknesses equivalent to a ground range of about 1500 m [50, 51]. Neutron cross-sections for ^{14}N and ^{16}O were newly evaluated for the computation of neutron transport through air. The resulting ENDF/B-VI evaluations turned out to be overall improvements over the previous evaluations, but they failed to remove the observed discrepancies, especially for Hiroshima [52]. Weather conditions at the time of the bombing were important for the transport calculation and were, therefore, scrutinized again. It was found that 'the DS86 atmospheric data are

not responsible for the observed discrepancy between measured and calculated radioactivity data (^{152}Eu and ^{60}Co) in Hiroshima' [53].

Thermoluminescence and neutron activation measurements on samples from Hiroshima and Nagasaki were continued. The thermoluminescence measurements in Hiroshima confirmed the discrepancies that had already been noted in the final report of DS86; new data were obtained for samples at larger distances from the hypocenter in Hiroshima than investigated in DS86, and they yielded ratios of measurement to calculation of about 2 at the largest distances (see e.g., [54]).

For neutron activation measurements, two approaches have been employed. The first one was to measure one radionuclide at different distances from the hypocenters. This approach had already been taken soon after the bombing for ^{32}P, and later for ^{60}Co and ^{152}Eu. Subsequently, additional data became available for ^{60}Co and ^{152}Eu at different distances from the hypocenter in Hiroshima (see e.g., [55–58]). These data, too, confirmed the discrepancies noted in the final report of DS86. In addition to a single measurement of ^{154}Eu published in 1983 [45], few further data were reported [59–61]. The most important new information resulted from the measurement of another radionuclide, ^{36}Cl, that was predominantly produced by thermal neutrons via a (n,γ) reaction on ^{35}Cl. It is a pure beta-emitter with a half-life of $3 \cdot 10^5$ years. The ^{36}Cl activities in Hiroshima and Nagasaki are far too low to be measured by counting techniques. In the late 1970s and early 1980s, however, the new technique of accelerator mass spectrometry (AMS) had been developed which turned out to be a powerful tool for the detection of long-lived radionuclides (see e.g., [62–64]). The first successful measurement of ^{36}Cl in Hiroshima was reported by Haberstock et al. [65], who investigated a granite gravestone that had been located 107 m from the hypocenter and measured activities substantially below the DS86 calculations. In the following years, systematic measurements were performed at different ground ranges in Hiroshima and confirmed the observed neutron discrepancy, measured ^{36}Cl activities at ground ranges of 1600 m being, as noted by Straume et al. [66], about 40 times larger than DS86 predictions. Figure 5 shows the available data which were summarized by Straume et al., together with data close to the hypocenter taken from Rühm et al. [49, 66].

At this point, it is interesting to put these discrepancies which were observed for radionuclides produced by thermal and epithermal neutrons in relation to ^{32}P, which was entirely produced by fast neutrons. Phenomenologically speaking, the dependence of the neutron fluence $F(r)$ from the slant range r can be described by $F(r) = F_1 \cdot e^{(-r/\lambda)}/r^2$ with the attenuation length λ. From DS86, the attenuation length λ_{DS86}(th) is obtained as λ_{DS86}(th) ≈ 139 m for thermal neutrons and λ_{DS86}(f) ≈ 212 m for fast neutrons. From thermal neutron activation measurements, an experimental attenuation lenght λ_{exp}(th) = 210 m can be derived for Hiroshima, taking data shown in Fig. 5. The experimental attenuation length λ_{exp}(f) for fast neutrons can be obtained from the ^{32}P data, using the Hamada re-evaluation [67] of the original data from Yamasaki and Sugimoto [17]. Figure 6 shows $r^2 \cdot A(^{32}\text{P})$ as a function of slant range r, with the ^{32}P activity A in disintegrations per minute and gram of sulfur. A least squares fit produces λ_{exp}(f) = 455 ± 143 m, which is statistically still compatible with the value of 212 m obtained in DS86. Since $(1/\lambda_{DS86}(\text{th})) - (1/\lambda_{exp}(\text{th})) \approx (1/\lambda_{DS86}(\text{f})) - (1/\lambda_{exp}(\text{f}))$, possible experimental corrections to DS86 neutron fluences as a function of distance from the hypocenter can be considered to be equal for thermal and for fast neutrons.

Similar discrepancies were not observed in Nagasaki, where the ^{36}Cl measurements were in agreement with DS86 calculations for ground ranges up to 1260 m, which put into doubt – as pointed out by Straume et al. [68] – the earlier measurements of ^{60}Co. The Nagasaki measurements indicate that there are no serious problems with the neutron transport calculations in air.

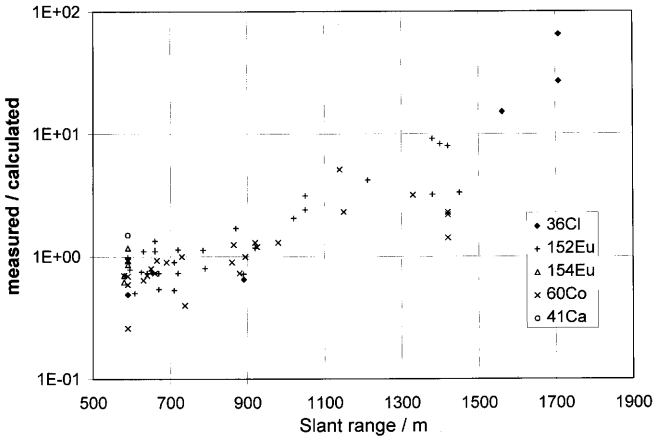

Fig. 5 Thermal neutron activation data normalized to calculated values, taken from Straume et al. [66] and Rühm et al. [49], as function of distance from the epicenter of Hiroshima

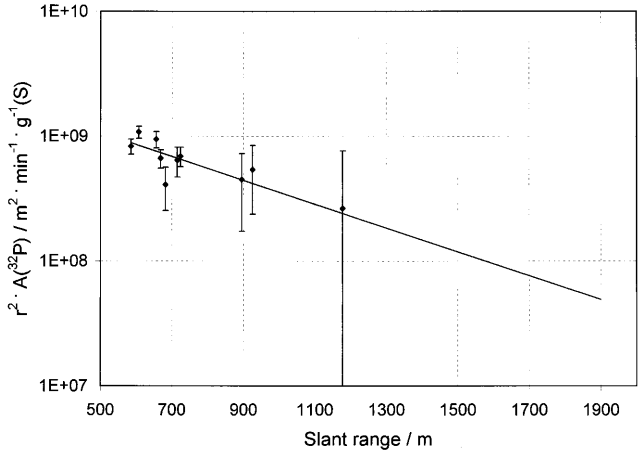

Fig. 6 ^{32}P activation data, based on the Hamada re-evaluation [67] of the original Yamasaki and Sugimoto data [17], as function of distance r from the epicenter of Hiroshima; $A(^{32}\text{P})$ denotes disintegrations per minute of ^{32}P per gram of sulfur at time of the bombing; *straight line* is a least squares fit

Table 1 Nuclides produced by neutrons from the A-bomb explosions and measured in samples from Hiroshima and Nagasaki (AMS accelerator mass spectrometry)

Nuclide	Half-life	Sample type	Ground range (m)	Method	Ref.
^{32}P	14.26 days	Electric power poles which contained sulfur used as an adhesive for insulators	76–1305	β-measurement	[16–18]
^{60}Co	5.272 y	e.g. reinforcing steel bars, granite, roof tiles	0–1295	γ-measurement	see e.g [31, 55–57]
^{152}Eu	13.33 y	Roof tiles, rock, concrete	0–1370	γ-measurement	see e.g. [45, 57–58, 61]
^{154}Eu	8.8 y	Rock, roof tiles, granite	0–132	γ-measurement	[45, 59–61]
^{36}Cl	$3.0 \cdot 10^5$ y	Granite, concrete	107–1606	AMS	[65–66, 72]
^{41}Ca	$1.03 \cdot 10^5$ y	Granite	107	AMS	[71, 73]
^{63}Ni	100 y	Steel	163	β-measurement	[83]

The second approach was to measure different radioisotopes at one location. It was, as stated above, applied in measurements on the granite gravestone 107 m from the hypocenter in Hiroshima. Various radionuclides produced by neutron activation were detected. ^{60}Co, ^{152}Eu, and ^{154}Eu were measured by gamma-spectroscopy [60, 69, 70]. In this gravestone, two further radioisotopes, ^{36}Cl and ^{41}Ca with half-lives of $3 \cdot 10^5$ years and 10^5 years, respectively, could be determined for the first time [65, 71–73]. The cross-sections of the (n,γ) reactions for these five radionuclides depend differently on energy – due to resonances in the epithermal energy region – which permitted an assessment of the energy spectrum of the neutrons at the location of the gravestone. The results for ^{41}Ca, ^{60}Co, ^{152}Eu, and ^{154}Eu were in accord with the energy spectrum that was predicted by DS86 for the location of the gravestone. The bomb yield thus inferred was 16 kt. However, when the ^{36}Cl data in the gravestone were included, a much harder neutron spectrum than the DS86 spectrum had to be assumed [49]. Table 1 shows all radionuclides which, up to now, have been identified in samples from Hiroshima and Nagasaki, together with corresponding half-lives, sample types, and ground ranges.

To summarize, recent neutron activation and thermoluminescence data confirmed the discrepancies for Hiroshima that had already been noted in the final report of DS86. Simultaneously, the ^{36}Cl activation measurements failed to confirm the discrepancy for Nagasaki which had also been noted in the final report of DS86. The findings suggest that the modelling of neutron and gamma-ray transport produces reasonable results and that the transport codes and cross-sections are reliable. Thus, the observed discrepancies might conceivably be due to unknown characteristics of the Hiroshima explosion. Since a similar device was never tested, some work was directed towards the investigation of the Hiroshima source terms. Whalen [74] pointed out that the comparison between calculated and measured values was poor for experiments with neutrons penetrating through iron material. This is of importance since in the Hiroshima bomb the prompt neutrons were primarily moderated by iron when penetrating through the casing. Whalen recommended the new ENDF/B-VI iron cross-section for recalculating the source terms of Hiroshima. Other authors observed that raising the height of the explosion or changing the directional distribution of the neutron leakage could not explain the observed discrepancies. However, a phenomenological source characterized by an arbitrary boost of neutrons emitted in the 2.1–2.7 MeV energy range and ±30 deg about the horizontal midplane of the bomb, together with complete elimination of neutrons above 2.7 MeV, could explain the observed neutron activation data with little change in gamma-dose. However, as stated by the authors of this study, 'a causal explanation for the boost is not available' [75]. Recently, similar studies were published by Hoshi et al. [76]. These authors found that by elevating the burst height about 90 m, assuming a 5% increase of the horizontal leakage of bare fission neutrons, and increasing the bomb yield about 20%, all neutron activation data and thermoluminescence gamma-ray data are simultaneously explained within 1 km ground range. Goldhagen et al. [77] compared calculations with neutron activation measurements performed at the U.S. Army Pulse Radiation Facility for distances from 300 m to nearly 2 km from a small unshielded fission reactor. These authors measured and calculated a similar fall-off of the thermal neutron fluence with distance compared to that for thermal neutrons at Hiroshima determined from activation measurements. They concluded that many more nearly unmoderated fission neutrons escaped from the Hiroshima weapon than were assumed in the DS86 model.

Options for further investigations

To resolve the neutron discrepancy in Hiroshima, added experimental and computational studies will be required, and in this connection it is desirable to explore further potential sources of information. Accordingly, radionuclides will be assessed here that have not been measured as yet, but can still provide information on the neutron fluence spectra in Hiroshima. The emphasis will be on the different reactions that lead to the production of the radionuclides by high- or low-energy neutrons, and on the resultant contributions from the A-bomb explosions relative to the contribution due to natural radioactivity in the samples or due to cosmic radiation. Except for ^{63}Ni, the production of the radionuclides will be discussed primarily in relation to the granitic gravestone. The sensitivity of the measure-

ment techniques will be considered with regard to the current potential of accelerator mass spectrometry or – in the case of ^{63}Ni and, especially, ^{39}Ar – of low level beta-counting. The methodology of chemical extraction of the various nuclides of interest is, of course, a central aspect of the investigations. Apart from a brief consideration of the extraction of ^{39}Ar from granite, this aspect will not be discussed here. As manifested by the sophisticated procedures that Straume and colleagues have developed for the preparation of ^{63}Ni samples [78–80], it would require a detailed treatment by itself.

Cross-sections that are relevant to the subsequent considerations are taken from the T-2 Nuclear Information Service at Los Alamos National Laboratory (LANL); this on-line service provides evaluated data from a variety of sources. In this paper, data were taken from the U.S. ENDF/B-VI library, the Japanese JENDL-3.2 library, and the Russian ADL-3T library. In addition, experimental data are also shown in the diagrams for comparison.

Calculation of the production of the discussed radionuclides is based on DS86 neutron spectra. It is noted that if the above-mentioned discrepancy for thermal neutrons and the attenuation length for fast neutrons deduced from the ^{32}P measurements were correct, the calculated production is expected to be higher.

Discussion of ^{63}Ni

Production

Shibata et al. [81] and Marchetti and Straume [82] have recently suggested the use of ^{63}Ni to estimate the fast neutron fluence of the Hiroshima A-bomb at ground level. Because of its half-life of 100 years, most of the ^{63}Ni nuclei produced after the A-bomb explosion are still extant today, more than 50 years after the explosion. Recently, ^{63}Ni was detected for the first time in a steel sample taken close to the hypocenter of Hiroshima. In this sample, ^{63}Ni had predominantly been produced by thermal neutrons [83]. In copper samples with low nickel content, however, ^{63}Ni is predominantly produced by fast neutrons via the reaction ^{63}Cu(n,p)^{63}Ni. Possible copper samples include lightning rods, rain gutters, wires, etc. The target isotope ^{63}Cu has an abundance of 69% in copper. ^{63}Ni is a pure beta-emitter with an endpoint energy of 70 keV. The Q value of the exothermic reaction is 0.7 MeV. However, Coulomb barrier effects (Coulomb barrier –4.9 MeV) assure that thermal activation of ^{63}Ni is negligible [81]. Figure 7 shows the (n,p) cross-section according to several data libraries. The cross-sections start to increase around 1 MeV; up to a neutron energy of about 4 MeV, the data of all libraries are largely consistent. Discrepancies occur above 4 MeV. Experimental data are limited and lie in the 14 MeV region [84–86], an exception being the recent data by Shibata et al. [87].

To assess the production of ^{63}Ni in copper samples exposed to the Hiroshima A-bomb explosion, DS86 neutron spectra such as those shown in Fig. 8 are used [41]. The

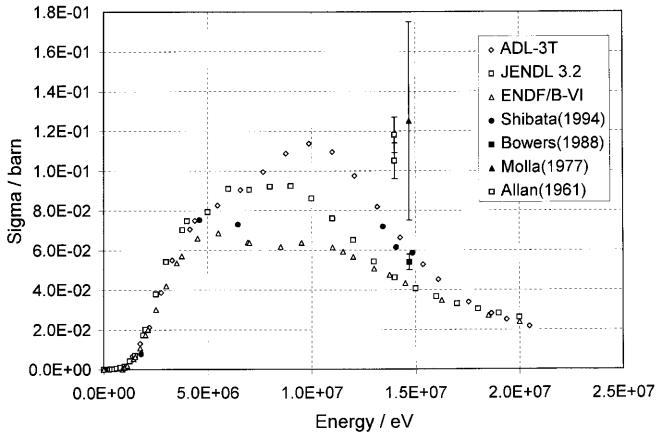

Fig. 7 Cross-section for the reaction ^{63}Cu(n,p)^{63}Ni as deduced from several cross-section libraries (ADL-3T, JENDL 3.2, ENDF/B-VI), compared to available experimental data [84–87]

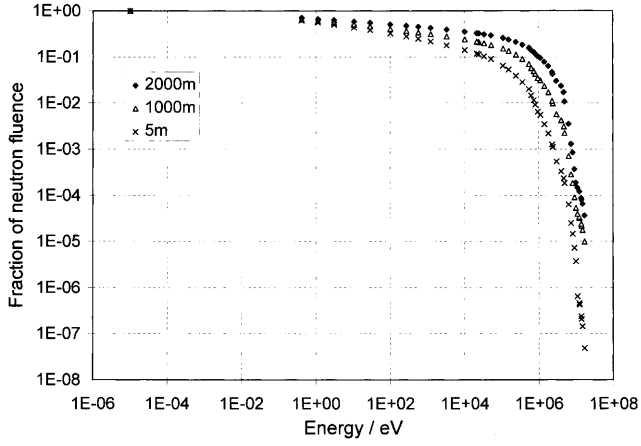

Fig. 8 DS86 neutron spectra (Hiroshima) for ground ranges of 5, 1000, and 2000 m, respectively, using an energy binning taken from DS86 [41]. Spectra are given in terms of fraction of fluence beyond specified energy

cross-sections in Fig. 7 were collapsed into the broad energy-group structure employed in DS86, using a 300K Maxwellian distribution of neutron energies below 0.125 eV and a 1/*E* distribution of neutron energies above 0.125 eV as weighting factors. They were then folded with the DS86 neutron spectrum close to the hypocenter, to derive the yield of ^{63}Ni in a 100 g copper sample. The resulting amounts were $1.7 \cdot 10^9$, $1.8 \cdot 10^9$, and $1.3 \cdot 10^9$ nuclei when the cross-sections from JENDL 3.2, ADL-3T, and ENDF/B-VI, respectively, were used. The calculated number of ^{63}Ni nuclei, thus, did not vary substantially, although the cross-sections differ at high energies. This is so because the cross-sections are similar between 1 and 4 MeV, while the DS86 neutron fluence is low for larger energies. Most of the ^{63}Ni is produced by neutrons between 1 and 5 MeV. This is illustrated in Fig. 9, which shows the fraction of ^{63}Cu(n,p)^{63}Ni activation beyond a specified energy for different ground ranges, using DS86 neutron spectra for Hiroshima and the ENDF/B-VI cross-section.

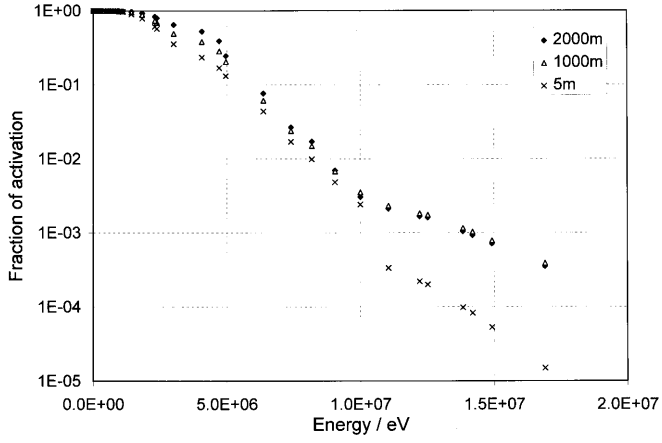

Fig. 9 Production of ^{63}Ni in Hiroshima via the reaction ^{63}Cu(n,p)^{63}Ni for different ground ranges and energies, given in terms of fraction of activation beyond specified energies. Activation was calculated on the basis of DS86 neutron fluences and ENDF/B-VI cross-section from Fig. 7

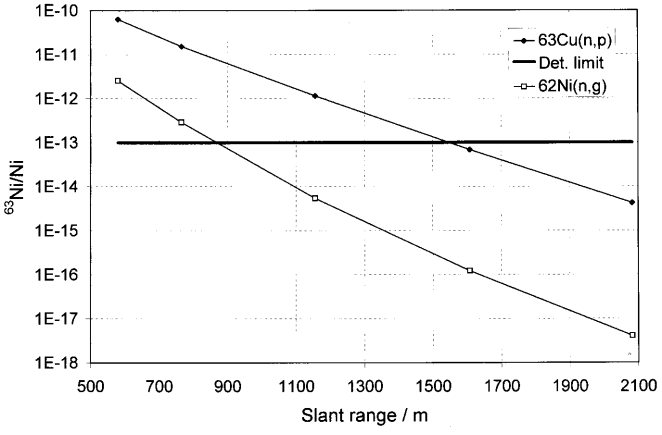

Fig. 10 Expected ^{63}Ni/Ni ratio in a copper sample with 19 ppm nickel impurity. Calculations were performed using DS86 neutron spectra, a bomb yield of 15 kt, and ENDF/B-VI cross-sections for the ^{63}Cu(n,p)^{63}Ni and ^{62}Ni(n,γ)^{63}Ni reactions. A detection limit extrapolated from ^{59}Ni results is shown for comparison [90]. Given slant ranges correspond to ground ranges of 5, 500, 1000, 1500 and 2000 m, respectively. *Lines between symbols* serve as eye guide

^{63}Ni can also be produced by thermal neutrons via the reaction ^{62}Ni(n,γ)^{63}Ni with a cross-section of about 15 barn. This contribution is proportional to the impurities of stable nickel (with 3.6% isotopic abundance of ^{62}Ni) in the copper sample.

For illustration, the production of ^{63}Ni was calculated, as described above, for a copper sample with the (n,p) cross-section taken from the ENDF/B-VI cross-section library and the DS86 neutron spectra at distances 5, 500, 1000, 1500, and 2000 m from the hypocenter (see Fig. 8 for examples). The results are given as the diamonds on the upper line in Fig. 10. The squares on the lower line give the contribution due to the ^{62}Ni(n,γ)^{63}Ni reaction, for these calculations a nickel impurity of 19 ppm is assumed, which was measured in a copper rain gutter from Hiroshima (McAninch JE, 1998, personal communication). It is seen in the figure that the concentration of ^{63}Ni produced by fast neutrons (diamonds) decreases by a factor of 1000 from the hypocenter to a distance of 1500 m. The contribution of the reaction ^{62}Ni(n,γ)^{63}Ni is insignificant for all distances. If, however, the nickel impurity was 500 ppm, the thermal neutrons would produce the same number of ^{63}Ni nuclei at the hypocenter via the (n,γ) reaction as fast neutrons via the (n,p) reaction.

Detection

Shibata et al. [81] suggested using low-level beta-counting for the detection of ^{63}Ni in Hiroshima samples. They estimated that in a 1 g copper sample exposed at 100 m from the hypocenter, the produced ^{63}Ni activity was $2.8 \cdot 10^{-3}$ Bq, and that a 2 g copper sample would be sufficient – at a background rate of 3.4 cpm in this counter and a detection efficiency of 55% – to produce a signal 3 sigma above background at a measuring time of 1000 min. The information so obtained could be valuable as an independent check of the ^{32}P data close to the hypocenter. However, the approach cannot provide information beyond 1000 m from the hypocenter, unless sample masses of about 1 kg are available. As stated earlier, the uncertainties of the ^{32}P data are large at this distance, while the discrepancies between thermal neutron activation measurements and DS86 calculations are highly significant.

Straume has emphasized the potentially important implications of the neutron discrepancy for the interpretation of the risk estimates on the basis of the data from Hiroshima [88, 89] and has pointed out that accelerator mass spectrometry (AMS) is a powerful tool to measure small amounts of long-living radionuclides that can be informative with regard to the neutron fluences. He also reported initial studies regarding the use of AMS for the determination of ^{63}Ni in Hiroshima samples [78]. He irradiated copper wires with fast neutrons from a ^{252}Cf source. After irradiation, nickel was extracted from the copper samples by use of electrolysis [79]. By means of a second chemical purification process, samples were transferred to the sample holders required for the AMS measurement [80]. This step employs the reaction of nickel with carbon monoxide to form nickel tetracarbonyl. ^{63}Ni was then measured by a combination of AMS and the detection of characteristic projectile x-rays. First results of this approach indicated that for a 95% confidence measurement near the hypocenter about 20 g of copper is required [78].

However, considerably higher sensitivity can be achieved. Recently, it was shown – in studies with ^{59}Ni – that AMS in combination with the use of a gas-filled analyzing magnet system (GAMS) can achieve detection limits that are about 2 orders of magnitude better than the detection limits for ^{63}Ni with the AMS and characteristic x-ray method [90]. Present and future activities will focus on the development of AMS with GAMS for ^{63}Ni. Extrapolating the background-limited detection limit for ^{59}Ni shows that with use of GAMS, a detection limit of ^{63}Ni/Ni

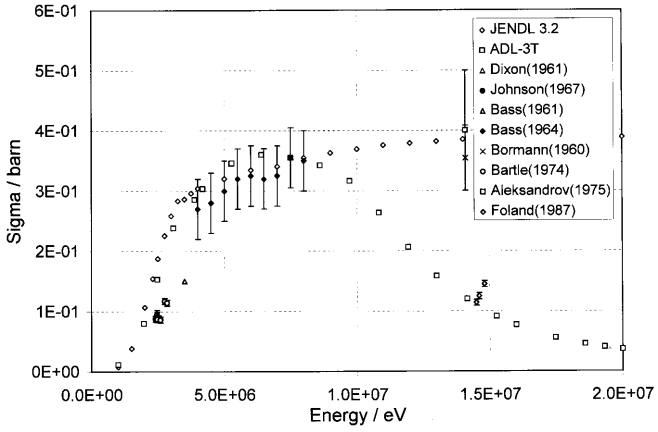

Fig. 11 Cross-sections for the reaction $^{39}K(n,p)^{39}Ar$ as deduced from several cross-section libraries (JENDL-3.2, ADL-3T), compared to available experimental data [91–98]

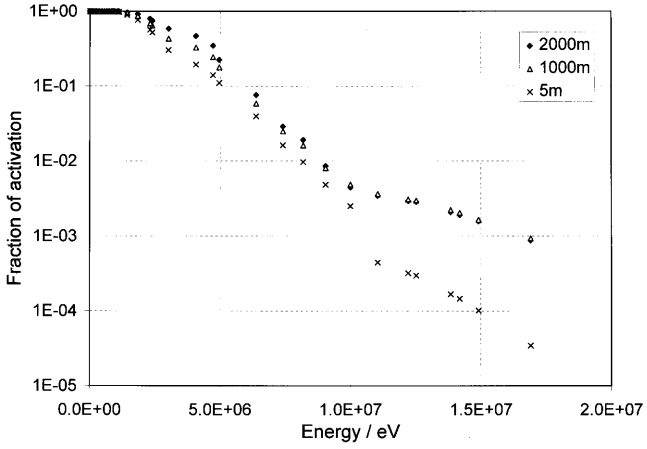

Fig. 12 Production of ^{39}Ar (Hiroshima) via the reaction $^{39}K(n,p)^{39}Ar$ for different ground ranges and energies, given in terms of fraction of activation beyond specified energies. Activation was calculated on the basis of DS86 neutron fluences and JENDL-3.2 cross-section from Fig. 11

of about 10^{-13} should be attainable, and this limit is, therefore, indicated in Fig. 10. Accordingly, it is expected that, close to the hypcenter, copper samples with a mass of less than 1 g are sufficient. These are estimates based on the DS86 neutron fluences. If the actual fluences are larger – in line with the present experimental evidence for thermal neutrons – measurements should be possible at even greater distances. However, the actual applicability of the method to samples, such as wires or gutters from Hiroshima, remains to be shown.

Discussion of ^{39}Ar

Production

A systematic search for possible threshold reactions showed that the reaction $^{39}K(n,p)^{39}Ar$ is another promising possibility for the detection of fast neutrons in Hiroshima [82], provided the argon has been trapped within a matrix without substantial leakage since 1945. A matrix which contains enough potassium and which has suitable retention/fixation characteristics is granite (Schultz L, 1998, personal communication). ^{39}Ar is a beta-emitter and has a half-life of 269 years and an endpoint energy of 0.6 MeV. The reaction is exothermic with Q = 0.2 MeV. Due to a Coulomb barrier of –3.4 MeV, thermal activation is expected to be negligible. The corresponding cross-sections, taken from several cross-section libraries, are shown in Fig. 11, together with measurements available in the literature [91–98]. At this point, it should be noted, however, that one publication reports a measurement at thermal energies of 32 ± 16 mb [99]. Taking again the DS86 neutron spectra (see Fig. 8 for examples) and assuming that activation by thermal neutrons is negligible, one finds that similarly to ^{63}Ni about 80% or more of the ^{39}Ar nuclei were produced by neutrons with energies between 1 and 5 MeV (Fig. 12). In this energy region, measurements do not agree well with the figures obtained from cross-section data files. Moreover, only a few measurements were made for these energies. Potential measurements of ^{39}Ar on Hiroshima and Nagasaki samples would, thus, have to be accompanied by cross-section measurements in the energy region between 1 and 5 MeV as well as at thermal energies.

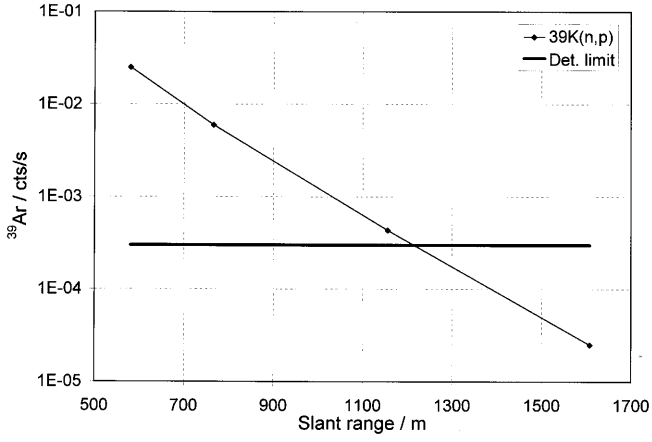

Fig. 13 Expected counting rates in 1998 due to neutron-induced ^{39}Ar activity, for a beta-detector efficiency of 60%. Calculations were performed using DS86 neutron spectra, a bomb yield of 15 kt, an evaluated cross-section taken from the JENDL-3.2 library, and a hypothetical gravestone sample of 100 g. A typical background counting rate is shown for comparison. Given slant ranges correspond to ground ranges of 5, 500, 1000, and 1500 m, respectively. *Line between symbols* serves as eye guide

A 100 g sample of the gravestone contains $3.6 \cdot 10^{22}$ atoms of ^{39}K (93.26% isotopic abundance of ^{39}K). Thus, with the cross-section from the JENDL-3.2 library, with a DS86 neutron spectrum for the distance 107 m from the hypocenter, and with a bomb yield of 15 kt, $5.5 \cdot 10^{8}$ nuclei of ^{39}Ar are estimated for a 100 g sample from the surface of the gravestone. In 1998, this corresponds to an activity of about 40 mBq, which could be registered by sophisticated low-level beta-counting techniques (see below). Figure 13 shows for a (hypothetical) 100-g sample

equal to that from the gravestone, the corresponding counting rates of ^{39}Ar at different distances from the epicenter assuming a counting efficiency of 60%; again, the DS86 neutron spectra (Fig. 8) and the cross-sections from the JENDL-3.2 library are used.

Production in granite by background reactions

Background production of radionuclides in the granite is due to natural radioactivity, i.e., due to neutrons originating either from spontaneous fission of ^{238}U or from alpha-decays of nuclides of the thorium and uranium decay series and subsequent (α,n) reactions, or due to cosmic rays that induce reactions either in situ, i.e., at the location of the quarry, or subsequently in the gravestone. The in situ production depends on shielding due to above-lying material and is, therefore, dependent on geologic erosion rates.

With the elemental composition of the granite [100] and with the neutron yields taken from Feige et al. [101], 4.2 neutrons are produced per g granite per year from the 0.95 ppm U and 4.4 ppm Th which have been measured in the granite. From this, and from a crude estimate of the production cross-section of 100 mb for typical neutron energies from the (α,n) reactions, a steady state concentration of about 23 atoms of ^{39}Ar per g granite can be estimated. The production of ^{39}Ar near the surface of the gravestone due to cosmic rays is estimated to be of the order of 200 atoms per year and per g potassium or calcium [102, 103]. After an estimated exposure age of 80 years of the gravestone and with the elemental composition of the granite, about 500 ^{39}Ar nuclei per g granite were produced at the surface. Earlier in situ production of ^{39}Ar in the granite can be neglected due to shielding at the location of the quarry and due to the short physical half-life.

Sample preparation and detection

The determination of noble gases in stone meteorites is a well established technique. Noble gases in chondrites are mixtures of different components. Radiogenic isotopes are produced by the decay of natural radionuclides such as ^{40}K or the isotopes of uranium and thorium. Cosmogenic nuclides are produced by the interaction of cosmic rays with meteoritic matter. Other gas components are trapped in meteorites, e.g., solar particles that are incorporated close to the surface. In order to extract noble gases from meteoritic material, typical sample masses of up to 150 mg are heated at about 100 °C for at least 1 day, to get rid of adsorbed rare gases of atmospheric origin. The samples are then heated in a tantalum oven at about 1700 °C for about 30 min. The completeness of gas extraction is checked by repeated heat-up. By use of a temperature-controlled charcoal trap the gases are separated cryogenically into three fractions: He plus Ne, Ar, and Kr plus Xe. For details, see for example [104, 105].

With regard to Hiroshima, measurements of ^{39}Ar are of interest, and then sample masses larger than 150 mg are needed (see Fig. 13). Work has been initiated to upgrade the experimental set-up for handling such large samples (Schultz L, 1998, personal communication).

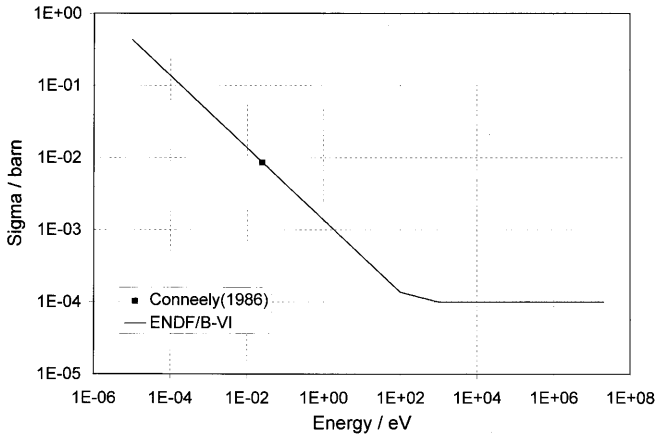

Fig. 14 ENDF/B-VI cross-section for the reaction ^{9}Be(n,γ)^{10}Be (*solid line*), compared to the result of the most recent experiment (*square*, 8.49 ± 0.34 mb, [107])

Typical background counting rates for high pressure proportional gas counters used in low-level laboratories to detect ^{39}Ar activities in groundwater samples are of the order of $3 \cdot 10^{-4}$ cts/s [106], (Loosli HH, 1998, personal communication). For a detector efficiency of 60%, a 10-g sample of the gravestone at a ground range of 107 m should lead to a counting rate in the detector which is about 7 times above the stated background counting rate. Figure 13 shows vs slant range the predicted counting rate in the detector due to ^{39}Ar for a 100-g sample. The diamonds on the line refer to close to the hypocenter, and to the distances 500, 1000, and 1500 m from the hypocenter. One infers that a 100-g sample 1500 m from the hypocenter could still produce a count rate of $3 \cdot 10^{-5}$ cts/s. For a practicable measuring time of 8 weeks, the background corrected result for the sample will then significantly differ from zero (on a 3 sigma statistical uncertainty). Therefore, with granite samples of masses up to 100 g, it appears possible to extend the measurements up to ground ranges of 1500 m. Suitable samples can be found, for example, as granite pebbles in concrete. Concrete itself is not suited, since it does not retain argon sufficiently.

Discussion of ^{10}Be

^{10}Be (half-life $1.6 \cdot 10^{6}$ years) is another radionuclide of interest. It was produced during the A-bomb explosions by the reactions ^{9}Be(n,γ)^{10}Be and ^{10}B(n,p)^{10}Be, the latter reaction being exothermic with Q = 0.2 MeV and Coulomb barrier –0.9 MeV. Figures 14 and 15 show for both reactions the cross-sections taken from the ENDF/B-VI library and experimental data from the literature [107, 108]. Figure 15 shows that the ENDF/B-VI cross-section of the (n,p)-reaction does not fit the experimental result of 6.4 ± 0.5 mb obtained by Lal et al. [108] for the neutron en-

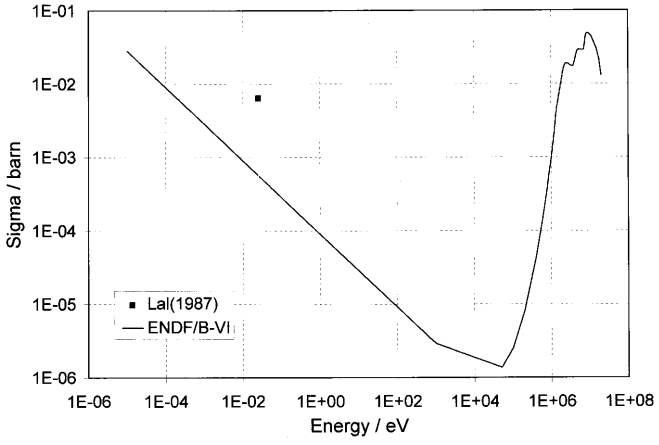

Fig. 15 ENDF/B-VI cross-section for the reaction $^{10}B(n,p)^{10}Be$ (*solid line*), compared to available experimental data (*square*, (6.4±0.5 mb, [108])

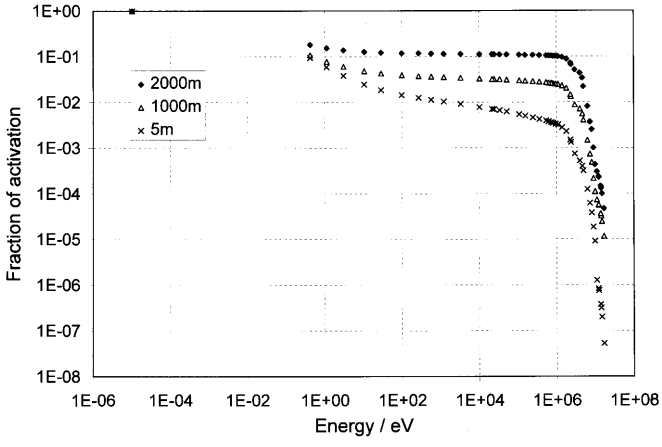

Fig. 16 Production of ^{10}Be in Hiroshima in a sample of the gravestone, for different ground ranges and energies. Activation by $^{9}Be(n,\gamma)^{10}Be$ and $^{10}B(n,p)^{10}Be$ is included, and given in terms of fraction beyond specified energies. Calculations were performed on the basis of DS86 neutron fluences and ENDF/B-VI cross-sections shown in Figs. 14 and 15. In the energy range from 10^{-5} to 10^{5} eV, the ENDF/B-VI cross-section for the (n,p) reaction is normalised to the experimental data given by Lal et al. [108] (Fig. 15)

ergy 25.3 meV. No further experimental data could be found for this reaction. Accordingly, in order to estimate the production of ^{10}Be from ^{10}B, the ENDF/B-VI cross-section curve was normalized in the energy range from 10^{-5} to 10^{5} eV to 6.4 mb at 25.3 meV.

For a 100-g sample of the gravestone (3 ppm B; 19.9% isotopic abundance of ^{10}B) with the DS86 neutron spectrum at a distance of 107 m from the hypocenter and cross-section as discussed above, one estimates, that about $1.5 \cdot 10^{5}$ atoms of ^{10}Be were produced by the reaction $^{10}B(n,p)^{10}Be$. A fraction of 3% is due to neutrons with energies in excess of 10^{5} eV. It is interesting to note that for a distance of 2000 m from the hypocenter, this fraction increases to almost 50% because of the hardening of the neutron spectrum. Via the reaction $^{9}Be(n,\gamma)^{10}Be$ and due to 3 ppm Be in the gravestone, about 10^{6} ^{10}Be nuclei were produced by thermal neutrons in a 100 g sample. Adding 0.5 mg Be as a carrier for the required chemistry results in a $^{10}Be/^{9}Be$ ratio of $3 \cdot 10^{-14}$ which is well above current detection limits of AMS facilities (see e.g., [109]). The reaction $^{13}C(n,\alpha)^{10}Be$ plays only a minor role because of its high threshold energy and low abundance of carbon in granite (see below). Figure 16 shows the fraction of ^{10}Be activation in the gravestone beyond specified energies, for the $^{10}B(n,p)^{10}Be$ and $^{9}Be(n,\gamma)^{10}Be$ reactions, and for different ground ranges in Hiroshima, based on DS86 neutron spectra and the cross-sections from above.

The production of ^{10}Be by neutrons from spontaneous fission of ^{238}U and due to the decay of the thorium and uranium series is minor. For the elemental composition of the gravestone [100] and with the production rate of 4.2 neutrons per g granite and year (see above), a steady-state concentration of about 3 atoms of ^{10}Be per g granite is inferred due to the reactions $^{9}Be(n,\gamma)^{10}Be$ and $^{10}B(n,p)^{10}Be$. In situ production of ^{10}Be in granite due to cosmic-ray-induced spallation and muon reactions can be estimated from information provided by Heisinger et al. [110]. The type of granite from which the gravestone was made has an age of about of 80 million years [111]. Typical erosion rates in the region of interest are estimated to be about 0.1 mm/year [112]. For these erosion rates, the saturation concentration for ^{10}Be in granite is about $4 \cdot 10^{4}$ nuclei per gram at the surface and about $5 \cdot 10^{3}$ nuclei per gram at a depth of 10 m [110] (Heisinger B, 1998, personal communication). For an estimated depth of 10–15 m of the original granite stone at the location of the quarry, the contribution of the in situ production is estimated to be less than 50% of the bomb signal. In the case of ^{10}Be, in situ production is therefore not negligible and has to be taken into account.

With an exposure age of about 80 years for the gravestone and with a production rate of 6 atoms of ^{10}Be per g granite and year at the surface [110], a background concentration of 480 atoms of ^{10}Be per g granite is estimated.

The measurement of ^{10}Be in the gravestone could provide an independent check of thermal neutrons at this site and could shed light on the discrepancy found for the activation of ^{41}Ca and ^{152}Eu, on the one hand, and of ^{36}Cl, on the other. Samples with high boron content but low beryllium content could yield additional information on the fast neutron fluence at large distances from the hypocenter. Materials that fullfill such requirements are being explored at present.

Discussion of ^{14}C

^{14}C with its half-life of 5730 years is a familiar radionuclide which can be measured by beta-counting and AMS. It is widely used for dating applications.

In the gravestone, ^{14}C was predominantly produced by the reactions $^{14}N(n,p)^{14}C$ and $^{17}O(n,\alpha)^{14}C$. The further reaction $^{13}C(n,\gamma)^{14}C$ can be disregarded in view of its small thermal cross-section and the low abundance of carbon in granite (typical values are 35–300 ppm [113]). Figure 17

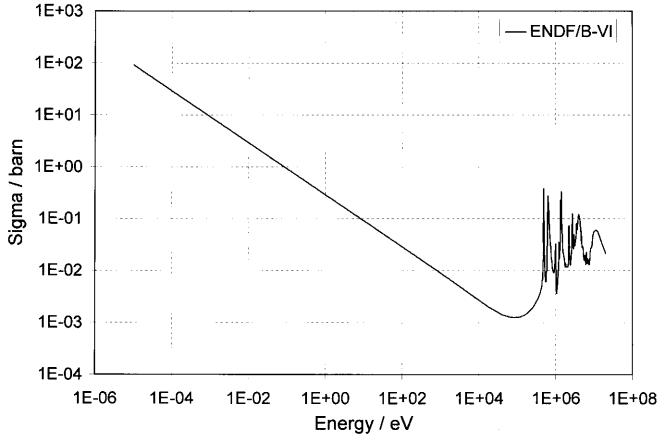

Fig. 17 ENDF/B-VI cross-section for the reaction $^{14}N(n,p)^{14}C$

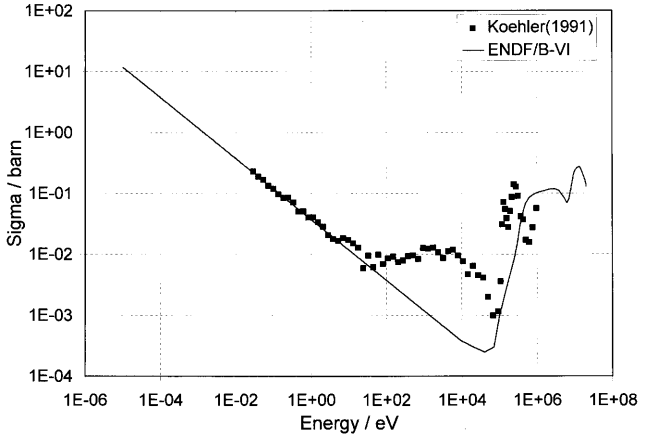

Fig. 18 ENDF/B-VI cross-section for the reaction $^{17}O(n,\alpha)^{14}C$ (*solid line*), compared to available experimental data (*squares*, [114])

shows the ENDF/B-VI cross-section for the $^{14}N(n,p)^{14}C$ reaction, which is well supported by many published measurements; the reaction is – through the interaction of secondary neutrons from cosmic rays with nitrogen of the atmosphere – the main source for the global ^{14}C inventory. For the second reaction, the ENDF/B-VI cross-section, as shown in Fig. 18, does not fit experimental data for energies larger than about 100 eV [114].

Typical concentrations of nitrogen in granite are of the order of 20 ppm [115]. For a 100-g sample of the gravestone, one estimates with the ENDF/B-VI cross-section in Fig. 17 and with the DS86 neutron spectrum at ground range 107 m about 10^9 atoms of ^{14}C due to the (n,p) reaction on nitrogen. A similar number of ^{14}C nuclei, i.e., $1.2 \cdot 10^9$, should be produced via the (n,α) reaction on oxygen. This was calculated on the basis of the measured oxygen mass abundance of about 50% in the granite, with 0.038% isotopic abundance of ^{17}O, and in terms of the measured cross-section for energies below 1 MeV measured by Koehler and Graff [114] and the ENDF/B-VI cross-section for energies above 1 MeV (Fig. 18). Even a carbon impurity of 300 ppm results in

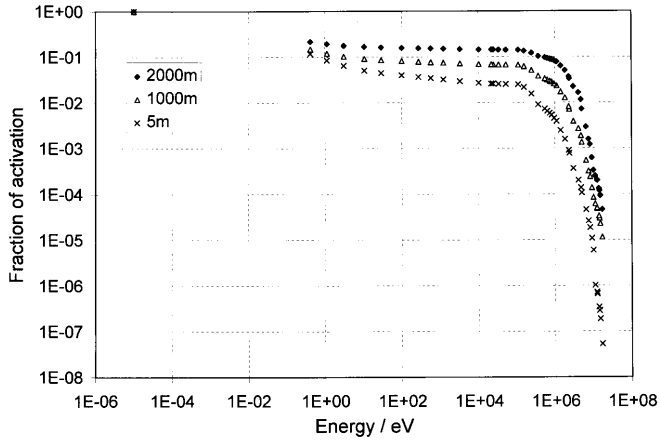

Fig. 19 Production of ^{14}C in Hiroshima in a sample of the gravestone, for different ground ranges and energies. Activation by $^{14}N(n,p)^{14}C$ and $^{17}O(n,\alpha)^{14}C$ is included, and given in terms of fraction beyond specified energies. Calculations were performed on the basis of DS86 neutron fluences and ENDF/B-VI cross-section shown in Fig. 17. The production via the (n,α) reaction was calculated using the experimental data given by Koehler et al. [114] for energies below 1 MeV, and the ENDF/B-VI cross-section for energies above that value (Fig. 18)

a $^{14}C/^{12}C$ ratio of about 10^{-12}, which is easily measured by AMS [109].

The steady-state concentration of ^{14}C due to reactions induced by the U and Th decay series is calculated to be 20 nuclei per g granite. As for in situ production due to cosmic radiation, the steady-state concentration is in the range of $7 \cdot 10^4$ ^{14}C nuclei per g granite at the surface. For an assumed depth of 10–15 m of the original granite at the location of the quarry, the steady-state concentration is about $3 \cdot 10^3$ ^{14}C nuclei per g granite. During an exposure period of 80 years at the graveyard and with a surface production rate of 20 nuclei per g quartz and year, 1600 nuclei of ^{14}C were produced per gram of the gravestone [110]. The background reactions are, thus, negligible compared with the bomb-induced signal.

It is interesting to note that about 7% of the nuclei produced by the $^{17}O(n,\alpha)^{14}C$ reaction are due to neutrons with energies larger than 65 eV. The fraction increases to about 25% at 2000 m from the hypocenter. Figure 19 shows the fraction of ^{14}C activation in the gravestone beyond specified energies, for the $^{14}N(n,p)^{14}C$ and $^{17}O(n,\alpha)^{14}C$ reactions, and for different ground ranges in Hiroshima, based on DS86 neutron spectra and the cross-sections from above. Calculations of the production of ^{14}C for other ground distances provide the dependence in Fig. 20 which shows that, for granitic samples with 300 ppm carbon content, ^{14}C can be detected up to distances of about 1000 m from the hypocenter.

Discussion of ^{59}Ni

Another radioisotope which could be measured in samples from Hiroshima and Nagasaki is ^{59}Ni. This radionuclide (half-life $1.08 \cdot 10^5$ years [116]) is mainly produced by

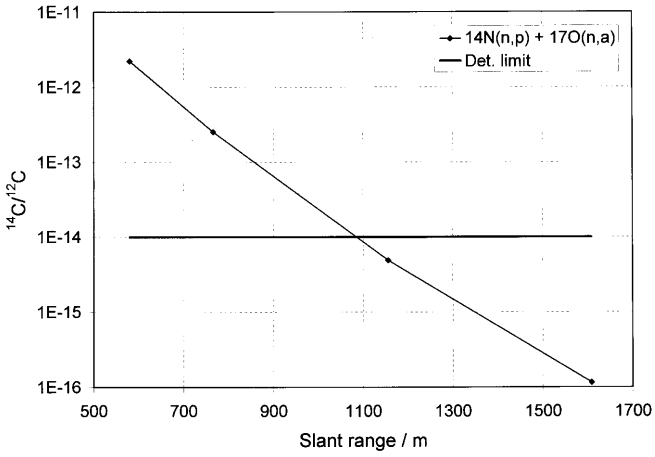

Fig. 20 Expected $^{14}C/^{12}C$ ratios taking production via $^{14}N(n,p)$ and $^{17}O(n,p)$ into account. Given ratios are calculated using DS86 neutron spectra. For the production via nitrogen, the cross-section of Fig. 17 is used. The production via oxygen was calculated by using the experimental data given by Koehler et al. [114] for energies below 1 MeV [118], and the ENDF/B-VI cross-section for energies above that value. Given ratios are for a sample from the gravestone assuming a nitrogen content of 20 ppm and a carbon content of 300 ppm. A typical detection limit of 10^{-14} is shown for comparison (even lower background levels were reported [109]). Given slant ranges correspond to ground ranges of 5, 500, 1000, and 1500 m, respectively. *Line between symbols* serves as eye guide

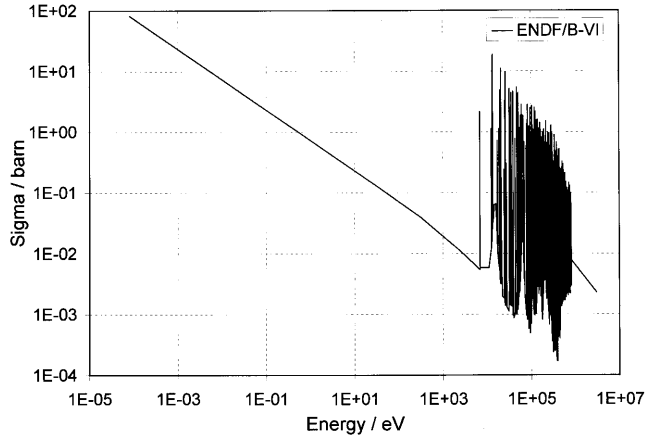

Fig. 21 ENDF/B-VI cross-section for the reaction $^{58}Ni(n,\gamma)^{59}Ni$

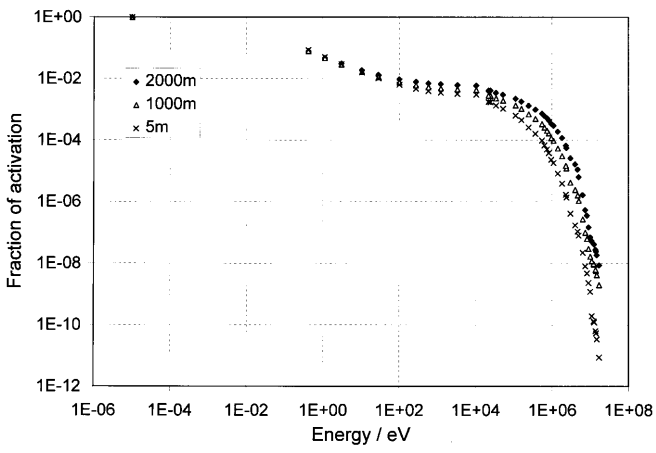

Fig. 22 Production of ^{59}Ni (Hiroshima) via the reaction $^{58}Ni(n,\gamma)^{59}Ni$ for different ground ranges and energies, given in terms of fraction of activation beyond specified energies. Calculations were performed on the basis of DS86 neutron fluences and ENDF/B-VI cross-section from Fig. 21

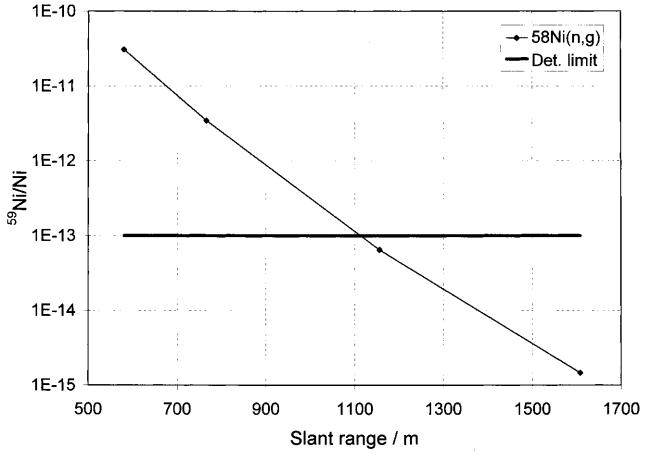

Fig. 23 Expected $^{59}Ni/Ni$ ratios for potential copper or gravestone samples without addition of nickel carrier, at different slant ranges. Given ratios are calculated using DS86 neutron spectra and ENDF/B-VI cross-section. A typical detection limit is shown for comparison [90]. Given slant ranges correspond to ground ranges of 5, 500, 1000, and 1500 m, respectively. *Line between symbols* serves as eye guide

thermal neutrons through the reaction $^{58}Ni(n,\gamma)^{59}Ni$. The cross-section decreases proportional to $1/v$, with a value of 4.6 b at 25 meV (Fig. 21), which is well established by measurements of several authors [117–119]. Additional experimental values for neutron energies in the keV and MeV region are given in [120–123]. The fact that ^{59}Ni is mainly produced by thermal neutrons is illustrated in Fig. 22, which shows the fraction of ^{59}Ni activation in the gravestone beyond specified energies, for the $^{58}Ni(n,\gamma)^{59}Ni$ reaction, and for different ground ranges in Hiroshima, based on DS86 neutron spectra and the corresponding ENDF/B-VI cross-section.

As a function of distance from the hypocenter, ratios of $^{59}Ni/Ni$ were calculated for the DS86 neutron spectra and with the cross-section in Fig. 21. These results are shown in Fig. 23 in relation to the detection limit $^{59}Ni/Ni = 10^{-13}$ which was published recently for the same experimental set-up that is to be employed for the detection of ^{63}Ni [90]. One concludes that ^{59}Ni could be detected up to a ground range of about 1000 m, provided no carrier needs to be added for sample preparation. It is interesting to note that in a 100-g copper sample with 19 ppm nickel impurity, about 2 mg nickel is present, which is enough to prepare an AMS sample. Any potential copper sample with 20 ppm nickel impurity or more offers, therefore, the possibility to measure – at ground ranges smaller than say 1000 m – both ^{59}Ni for an estimate of the thermal neutron fluence and ^{63}Ni for an estimate of the fast neutron fluence.

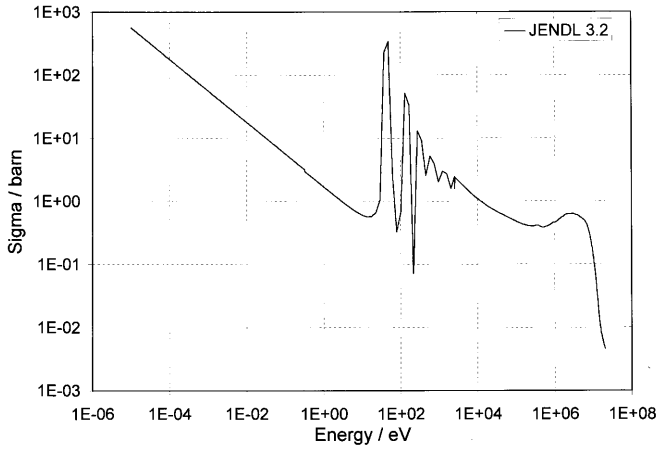

Fig. 24 JENDL 3.2 cross-section for the reaction $^{130}Ba(n,\gamma)^{131}Ba$

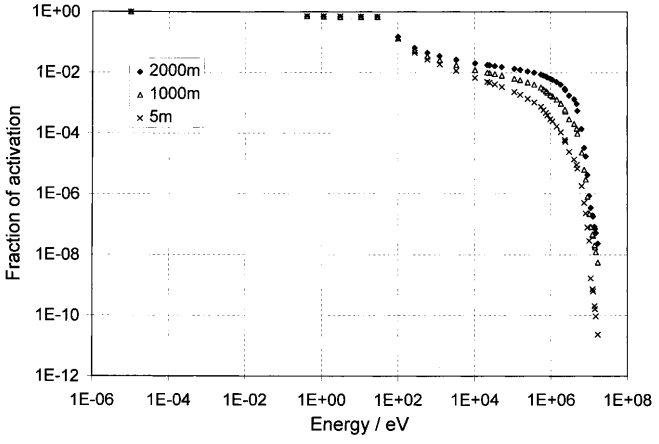

Fig. 25 Production of ^{131}Xe (Hiroshima) for different ground ranges and energies, given in terms of fraction of activation beyond specified energies. Calculations were performed on the basis of DS86 neutron fluences and ENDF/B-VI cross-section from Fig. 24

For the gravestone, a ratio of $^{59}Ni/Ni = 2.1 \cdot 10^{-11}$ is estimated. Since the Ni content of the gravestone is about 2 ppm, about $3.6 \cdot 10^7$ atoms of ^{59}Ni were produced in a 100-g sample. Even if 1 mg carrier is necessary for chemical extraction, the resulting ratio $^{59}Ni/Ni = 2 \cdot 10^{-12}$ is well above the established detection limit (see above).

Discussion of ^{131}Xe

Following the Apollo missions in the late 1960s, studies of lunar rocks revealed anomalously high isotopic fractions of stable ^{131}Xe. This isotope is produced via neutron capture from ^{130}Ba with two subsequent β^- decays. The high abundance of ^{131}Xe was subsequently explained by a large (n,γ) cross-section for epithermal energies. Measurements of this cross-section were performed by Kaiser and Berman [124]. Figure 24 shows the (n,γ) cross-section, which is characterized by pronounced resonances in the epithermal energy region. With this cross-section and with the DS86 neutron spectrum close to the hypocenter, $1.6 \cdot 10^8$ atoms of ^{131}Xe should have been produced in a 100-g sample of the granite gravestone. Some 65% of the ^{131}Xe nuclei were produced by neutrons with energies between 29 and 275 eV (Fig. 25). Therefore, ^{131}Xe could be a monitor for epithermal neutrons in Hiroshima (Y. Shukolyukov, 1998, personal communication). In the gravestone, ^{131}Xe can be detected by use of conventional mass spectrometry. The feasibility of ^{131}Xe as a neutron monitor in Hiroshima granite depends crucially, however, on the content of atmospheric xenon in the granite. Preliminary studies are presently aimed at the investigation of the potential use of ^{131}Xe as a neutron monitor for Hiroshima.

Conclusion

The thermal neutron discrepancy of Hiroshima was first noted in the final report of the current dosimetry system DS86. It was subsequently confirmed by a number of investigators. ^{63}Ni and ^{39}Ar are the two radionuclides that were generated by fast neutrons and that can, even today, be measured to obtain added information on the fast neutron fluence from the A-bomb explosion in Hiroshima. It is shown that recent developments will – in the near future – allow measurements on samples up to ground ranges of about 1500 m from the hypocenter. The results of these measurements should contribute to the resolution of the neutron discrepancy and, thereby, to improved estimates of the neutron doses to the A-bomb survivors in Hiroshima. While there is no apparent neutron discrepancy in Nagasaki, similar measurements may still be valuable in ascertaining the agreement between computations and measurements in this city.

The earlier simultaneous measurements of ^{36}Cl, ^{41}Ca, ^{60}Co, ^{152}Eu, and ^{154}Eu in granite from a gravestone indicated that the neutron spectrum close to the hypocenter of Hiroshima may have been harder than assumed in DS86. It has, therefore, been suggested here to measure further radionuclides, such as ^{10}Be, ^{14}C, ^{39}Ar, ^{59}Ni, and potentially ^{131}Xe, in the same sample. Two of these nuclides, ^{10}B and ^{59}Ni, are almost exclusively produced by thermal neutrons. Some 3.5% of the ^{14}C is produced by neutrons with energies in excess of 65 eV. ^{131}Xe is predominantly produced by epithermal neutrons. ^{39}Ar is produced mainly by fast neutrons, if the DS86 neutron spectrum is assumed. The proposed set of ten radionuclides should provide, if measured in the same sample, very firm information on the neutron spectrum close to the hypocenter.

References

1. Roesch WC (ed) (1987) US-Japan joint reassessment of atomic bomb radiation dosimetry in Hiroshima and Nagasaki – final report. Radiation Effects Research Foundation, Vols. 1 and 2, Hiroshima, Japan
2. Auxier JA (1977) ICHIBAN – Radiation dosimetry for the survivors of the bombings of Hiroshima and Nagasaki. (ERDA Critical Review Series, TID-27080) Department of Energy, Washington, D.C.

3. Kerr GD, Hashizume T and Edington CW (1987) Historical review. In: US-Japan joint reassessment of atomic bomb radiation dosimetry in Hiroshima and Nagasaki – final report 1. Radiation Effects Research Foundation, Hiroshima, pp1–13
4. Pfennig G, Klewe-Nebenius H, Seelmann-Eggebert W (1995) Karlsruher Nuklidkarte – Chart of the Nuclides. Forschungszentrum Karlsruhe
5. Firestone RB (1996) Table of isotopes, 8th edn. Wiley, New York
6. Kimura K, Tajima E (1953) Location of A-bomb explosion and size of the fireball. (Collection of Investigative Reports on Atomic Bomb Disaster) Science Council of Japan, Tokyo, pp 3–87
7. Uda K, Sugahara Y, Kita I. (1953) Meteorological conditions related to the atomic bomb explosions in Hiroshima. (Collection of Investigative Reports on Atomic Bomb Disaster) Science Council of Japan, Tokyo, pp 98–136
8. Shinohara K, Morita A, Kora K, Kawai N and Yokota M (1953) Radioactivity of the ground in Nagasaki city and vicinity. (Collection of Investigative Reports on Atomic Bomb Disaster) Science Council of Japan, Tokyo, pp 45–53
9. Tybout RA (1946) Radiation in Hiroshima and Nagasaki. (Technical Report WO-170) US Atomic Bomb Energy Commission
10. Pace N, Smith RE (1959) Measurement of the residual radiation intensity at the Hiroshima and Nagasaki bomb sites. (Technical report) Atomic Bomb Casualty Commission, Hiroshima, pp 26–59
11. Fujiwara T, Takeyama H (1953) Residual radioactivity around Hiroshima city. (Collection of Investigative Reports on Atomic Bomb Disaster) Science Council of Japan, Tokyo, pp 75–83
12. Miyasaki T, Ikeda M (1953) A-bomb radiation in Hiroshima city and vicinity (1). (Collection of Investigative Reports on Atomic Bomb Disaster) Science Council of Japan, Tokyo, pp 34–35
13. Miyasaki T, Masuda T (1953) A-bomb radiation in Hiroshima city and vicinity (2). (Collection of Investigative Reports on Atomic Bomb Disaster) Science Council of Japan, Tokyo, pp 35–38
14. Kimura M (1953) Measurement of radiation near the hypocenter at Hiroshima by Lauritsen electroscope. (Collection of Investigative Reports on Atomic Bomb Disaster) Science Council of Japan, Tokyo, pp 40–41
15. Shinohara K, Okada T, Morita A, Inoue K (1953) Radioactivity of the ground in Nagasaki city and vicinity. I. Radioactivity near the hypocenter. (Collection of Investigative Reports on Atomic Bomb Disaster) Science Council of Japan, Tokyo, pp 41–44
16. Arakatsu B (1953) Report on survey of radioactivity in Hiroshima several days after the atomic bomb explosion. (Collection of Investigative Reports on Atomic Bomb Disaster) Science Council of Japan, Tokyo, pp 5–10
17. Yamasaki F, Sugimoto A (1953) Radioactive ^{32}P produced in sulfur in Hiroshima. (Collection of Investigative Reports on Atomic Bomb Disaster) Science Council of Japan, Tokyo, pp 18–19
18. Sugimoto A (1953) Determination of number of fast neutron particles emitted at the time of the Hiroshima A-bomb explosion. (Collection of Investigative Reports on Atomic Bomb Disaster) Science Council of Japan, Tokyo, p 19
19. Liebov AA (1965) A medical diary of Hiroshima, 1945. Yale J Biol Med 38:61–239
20. Jungk R (1970) Brighter than a thousand suns. Harcourt, Brace and Jovanovich, New York
21. Shimizu S (1982) Historical sketch of the scientific field survey in Hiroshima several days after the atomic bombing. Bull Inst Chem Res Kyoto Univ 60 (2)
22. Cogan DG, Martin SF, Kimura SJ (1949) Atom bomb cataracts. Science 110:654–655
23. Cogan DG, Martin SF, Kimura SJ, Ikui H (1950) Opthalmologic survey of atomic bomb survivors in Japan. Trans Am Opthalmol Soc 48:62–87
24. Foley JH, Borges W, Yamawaki T (1952) Incidence of leukemia in survivors of the atomic bomb in Hiroshima and Nagasaki. Jpn Am J Med 13:311–321
25. Moloney WC, Lange RD (1954) Leukemia in atomic bomb survivors. II. Observations on early phases of leukemia. Blood 9:663–685
26. Auxier JA, Cheka JS, Haywood FF, Jones TD, Thorngate JH (1966) Free-field radiation-dose distributions from the Hiroshima and Nagasaki bombings. Health Phys 12:425–429
27. Arakawa ET (1960). Radiation dosimetry in Hiroshima and Nagasaki atomic-bomb survivors. N Engl J Med 263:488–493
28. Milton RC, Shohoji T (1968) Tentative 1965 radiation dose estimation for atomic bomb survivors. (Technical report TR 1-68) Atomic Bomb Casualty Commission, Hiroshima and Nagasaki
29. Higashimura T, Ichikawa Y, Sidei T (1963) Dosimetry of atomic bomb radiation in Hiroshima by thermoluminescence of roof tiles. Science 139:1284–1285
30. Ichikawa Y, Higashimura T, Sidei T (1966) Thermoluminescence dosimetry of gamma rays from atomic bombs in Hiroshima and Nagasaki. Health Phys 12:395–405
31. Hashizume T, Maruyama T, Shiragai A, Tanaka E, Izawa M, Kawamura S, Nagaoka S (1967) Estimation of the air dose from the atomic bombs in Hiroshima and Nagasaki. Health Phys 13:149–161
32. Saito N (1961) Annual report of scientific research grants, radiation section. Co-operative Res 13:142–143
33. Kawamura S, Izawa M, Maruyama T, Tanaka E, Hashizume M (1967) Determination of ^{60}Co to Co ratio for the estimation of fast neutron dose from the atomic bombs in Hiroshima and Nagasaki. Health Phys 13:801–806
34. Rossi HH, Mays CW (1978) Leukemia risk from neutrons. Health Phys 34:353–360
35. Rossi HH, Kellerer AM (1974) The validity of risk estimates of leukemia incidence based on Japanese data. Radiat Res 58:131–140
36. Marshall E (1981a) New A-bomb studies alter radiation estimates. Science 212:900–903
37. Marshall E (1981b). New A-bomb data shown to radiation experts. Science 212:1364–1365
38. Loewe WE, Mendelsohn E (1981) Revised dose estimates at Hiroshima and Nagasaki. Health Phys 41:663–666
39. Malik J, Tajima E, Binninger G, Kaul DC, Kerr GD (1987) Yields of the bombs. In: US-Japan joint reassessment of atomic bomb radiation dosimetry in Hiroshima and Nagasaki – final report 1. Radiation Effects Research Foundation, Hiroshima, pp 26–36
40. Whalen PP (1987) Calculation and verification of source terms. In: US-Japan joint reassessment of atomic bomb radiation dosimetry in Hiroshima and Nagasaki – final report 1. Radiation Effects Research Foundation, Hiroshima, pp 37–65
41. Kerr GD, Pace JV III, Mendelsohn E, Loewe WE, Kaul DC, Dolatshahi F, Egbert SD, Gritzner M, Scott WH Jr, Marcum J, Kosako T, Kanda K (1987) Transport of initial radiations in air over ground. In: US-Japan joint reassessment of atomic bomb radiation dosimetry in Hiroshima and Nagasaki – final report 1. Radiation Effects Research Foundation, Hiroshima, pp 66–142
42. Christy RF, Tajima E (1987) Executive summary. In: US-Japan joint reassessment of atomic bomb radiation dosimetry in Hiroshima and Nagasaki – final report 1. Radiation Effects Research Foundation, Hiroshima, pp 14–25
43. Maruyama T, Kumamoto Y, Ichikawa Y, Nagatomo T, Hoshi M, Haskell E, Kaipa P (1987) Thermoluminescence measurements of gamma rays. In: US-Japan joint reassessment of atomic bomb radiation dosimetry in Hiroshima and Nagasaki – final report 1. Radiation Effects Research Foundation, Hiroshima, pp 143–184
44. Sakanoue M, Maruo Y, Komura K (1981) In-situ low-level gamma-ray spectrometry and x-ray fluorescence analysis. In: Int. Symp. Meth. low-level counting and spectrometry. (STI/PUB/592) International Atomic Energy Agency, Vienna, pp 105–124

45. Nakanishi T, Imura T, Komura K, Sakanoue M (1983) ^{152}Eu in samples exposed to the nuclear explosions at Hiroshima and Nagasaki. Nature 302: 132–134
46. Loewe EW (1985) Hiroshima and Nagasaki initial radiations: delayed neutron contributions and comparison of calculated and measured cobalt activations. Nucl Technol 68: 311–318
47. Loewe WE, Mendelsohn E, Hamada T, Maruyama T, Okajima S, Pace JV III, Sakanoue M, Kondo S, Hashizume T, Marcum J, Woolson WA (1987) Measurements of neutron fluences. In: US-Japan joint reassessment of atomic bomb radiation dosimetry in Hiroshima and Nagasaki – final report 1. Radiation Effects Research Foundation, Hiroshima, pp 185–204
48. Kaul DC, Woolson WA, Egbert SD, Straume T (1994) A brief summary of comparisons between the DS86 A-bomb survivor dosimetry system and in-situ measurements in light of new measurements, revised nuclear data and improved calculational methods. Proceedings of the 8th International Conference on Radiation Shielding, Arlington, Texas, pp 232–237
49. Rühm W, Kato K, Korschinek G, Morinaga H, Nolte E (1995) Neutron spectrum and yield of the Hiroshima A-bomb deduced from radionuclide measurements at one location. Int J Radiat Biol 68: 97–103
50. Hoshi M, Hiraoka M, Hayakawa N, Sawada S, Munaka M, Kuramoto A, Oka T, Iwatani K, Shizuma K, Hasai H, Kobayashi T (1992) Benchmark test of transport calculations of gold and nickel activation with implications for neutron kerma at Hiroshima. Health Phys 63: 532–541
51. Iwatani K, Hoshi M, Shizuma K, Hiraoka M, Hayakawa N, Oka T, Hasai H (1994) Benchmark test of neutron transport calculations: indium, nickel, gold, europium, and cobalt activation with and without energy moderated fission neutrons by iron simulating the Hiroshima atomic bomb casing. Health Phys 67: 354–362
52. Hale GM, Young PG, Chadwick MB, Chen ZP (1994) R-matrix analysis for nitrogen and oxygen. Proceedings of the 8th International Conference on Radiation Shielding, Arlington, Texas, pp 224–231
53. Hoshi M, Sawada S, Nagatomo T, Neyama Y, Marumoto K, Kanemaru K (1992) Meteorological observations at Hiroshima on days with weather similar to that of the atomic bombing. Health Phys 63: 656–664
54. Nagatomo T, Hoshi M, Ichikawa Y (1995) Thermoluminescence dosimetry of the Hiroshima atomic-bomb gamma rays between 1.59 km and 1.63 km from the hypocenter. Health Phys 69: 556–559
55. Kimura T, Takano N, Iba T, Fujita S, Watanabe T, Maruyama T, Hamada T (1990) Determination of specific activity of cobalt (^{60}Co/Co) in steel samples exposed to the atomic bomb in Hiroshima. J Radiat Res 31: 207–231
56. Shizuma K, Iwatani K, Hashi H, Oka T, Morishima H, Hoshi M (1992) Specific activities of 60Co and 152Eu in samples collected from the atomic-bomb dome in Hiroshima. J Radiat Res 33: 151–162
57. Shizuma K, Iwatani K, Hasai H, Hoshi M, Oka T, Morishima H (1993) Residual ^{152}Eu and ^{60}Co activities induced by neutrons from the Hiroshima atomic bomb. Health Phys 65: 272–282
58. Shizuma K, Iwatani K, Hasai H, Hoshi M, Oka T (1997) ^{152}Eu depth profiles in granite and concrete cores exposed to the Hiroshima atomic bomb. Health Phys 72: 848–855
59. Hasai H, Iwatani K, Shizuma K, Hoshi M, Yokoro K, Sawada S, Kosako T, Morishima H (1987) Europium-152 depth profile of a stone bridge pillar exposed to the Hiroshima atomic bomb: ^{152}Eu activities for analysis of the neutron spectrum. Health Phys 53: 227–239
60. Rühm W, Kato K, Korschinek G, Morinaga H, Urban A, Zerle L, Nolte E (1990) The neutron spectrum of the Hiroshima A-bomb and the Dosimetry System 1986. Nucl Instr Methods B52: 557–562
61. Nakanishi T, Ohtani H, Mizuochi R, Miyaji K, Yamamoto T, Kobayashi K, Imanaka T (1991) Residual neutron-induced radionuclides in samples exposed to the nuclear explosion over Hiroshima: comparison of the measured values with the calculated values. J Radiat Res [Suppl] 69–82
62. Purser KH, Liebert RB, Litherland AE, Beukens RP, Gove HE, Bennett CL, Clover MR, Sondheim WE (1977) An attempt to detect stable N^- ions from a sputter ion source and some implications of the results for the design of tandems for ultra-sensitive carbon analysis. Revue Phys Appl 12: 1487–1492
63. Elmore D, Tubbs LE, Newman D, Ma XZ, Finkel R, Nishiizumi K, Beer J, Oeschger H, Andree M (1982) ^{36}Cl bomb pulse measured in a shallow ice core from Dye 3, Greenland. Nature 300: 735–737
64. Kubik P, Korschinek G, Nolte E (1983) Accelerator mass spectrometry with completely stripped ^{36}Cl at the Munich postaccelerator. Nucl Instr Methods B1: 51–59
65. Haberstock G, Heinzl J, Korschinek G, Morinaga H, Nolte E, Ratzinger U, Kato K, Wolf M (1986) Accelerator mass spectrometry with fully stripped ^{36}Cl ions. Radiocarbon 28: 204–210
66. Straume T, Egbert SD, Woolson WA, Finkel RC, Kubik RC, Gove HE, Sharma P, Hoshi M (1992) Neutron discrepancies in the DS86 Hiroshima Dosimetry System. Health Phys 63: 412–426
67. Hamada T (1983) Measurements of ^{32}P activity induced in sulfur in Hiroshima. In: US-Japan joint workshop for reassessment of atomic bomb radiation dosimetry in Hiroshima and Nagasaki, pp 45–56
68. Straume T, Harris LJ, Marchetti AA and Egbert SD (1994) Neutrons confirmed in Nagasaki and at the Army Pulsed Radiation Facility: implications for Hiroshima. Radiat Res 138: 193–200
69. Kato K, Habara M, Aoyama T, Yoshizawa Y, Biebel U, Haberstock G, Heinzl J, Korschinek G, Morinaga H, Nolte E (1988) Measurements of neutron fluence from the Hiroshima atomic bomb. J Radiat Res 29: 261–266
70. Kato K, Habara M, Aoyama T, Yoshizawa Y (1990) Gamma-ray measurements of ^{152}Eu produced by neutrons from the Hiroshima atomic bomb and evaluation of neutron fluence. Jpn J Appl Phys 29: 1546–1549
71. Korschinek G, Morinaga H, Nolte E, Preisenberger E, Ratzinger U, Urban A, Dragovitsch P, Vogt S (1987) Accelerator mass spectrometry with completely stripped ^{41}Ca and ^{53}Mn ions at the Munich tandem accelerator. Nucl Instr Methods B29: 67–71
72. Kato K, Habara M, Yoshizawa Y, Biebel U, Haberstock G, Heinzl J, Korschinek G, Morinaga H, Nolte E (1990) Accelerator mass spectrometry of ^{36}Cl produced by neutrons from the Hiroshima bomb. Int J Radiat Biol 58: 661–672
73. Rühm W, Kato K, Korschinek G, Morinaga H, Nolte E (1992) ^{36}Cl and ^{41}Ca depth profiles in a Hiroshima granite stone and the Dosimetry System 1986. Z Phys A Hadrons and Nuclei 341: 235–238
74. Whalen PP (1994) Source and replica calculations. Proceedings of the 8th International Conference on Radiation Shielding, Arlington, Texas, pp 212–223
75. Rhoades WA, Barnes JM, Santoro RT (1994) An explanation of the Hiroshima activation dilemma. Proceedings of the 8th International Conference on Radiation Shielding, Arlington, Texas, pp 238–244
76. Hoshi M, Takada J, Endo S, Shizuma K, Iwatani K, Oka T, Fujita S, Hasai H (1998) Problems of radiation dose evaluation in Hiroshima and Nagasaki and their explanation. Radiat Prot Dosim 77: 15–23
77. Goldhagen P, Reginatto M, Hajnal F (1996) Neutron spectrum measurements at distances up to 2 km from a uranium fission source for comparison with transport calculations. In: Proc Am Nucl Soc Topical Meeting Radiation Protection and Shielding. American Nuclear Society, La Grange Park, Ill., pp 139–146
78. Straume T, Marchetti AA, McAninch JE (1996) New analytical capability may provide solution to the neutron dosimetry problem in Hiroshima. Radiat Prot Dosim 67: 5–8
79. Marchetti AA, Hainsworth LJ, McAninch JE, Leivers MR, Jones PR, Proctor ID, Straume T (1997) Ultra-separation of nickel from copper metal for the measurement of ^{63}Ni by AMS. Nucl Instr Methods Phys Res B 123: 230–234

80. McAninch JE, Hainsworth LJ, Marchetti AA, Leivers MR, Jones PR, Dunlop AE, Mauthe R, Vogel JS, Proctor ID, Straume T (1997) Measurement of ^{63}Ni and ^{59}Ni by accelerator mass spectrometry using characteristic projectile X-rays. Nucl Instr Methods Phys Res B 123: 137–143
81. Shibata T, Imamura M, Shibata S, Uwamino Y, Ohkubo T, Satoh S, Nogawa N, Hasai H, Shizuma K, Iwatani K, Hoshi M, Oka T (1994) A method to estimate the fast-neutron fluence for the Hiroshima atomic bomb. J Phys Soc Jpn 63: 3546–3547
82. Marchetti AA, Straume T (1996) A search for neutron reactions that may be useful for Hiroshima dose reconstruction. Appl Radiat Isot 47: 97–103
83. Shizuma K, Iwatani K, Hasai H, Oka T, Hoshi M, Shibata S, Imamura M, Shibata T (1997) Identification of ^{63}Ni and ^{60}Co produced in a steel sample by thermal neutrons from the Hiroshima atomic bomb. Nucl Instr Methods Phys Res A 384: 375–379
84. Bowers DL, Greenwood LR (1988) Analysis of long-lived isotopes by liquid scintillation spectrometry. J Radioanal Nucl Chem 123: 461–469
85. Molla NI, Qaim SM (1977) A systematic study of (n,p) reactions at 14.7 MeV. Nucl Phys A283: 269–288
86. Allan DL (1961) An experimental test of the statistical theory of nuclear reactions. Nucl Phys 24: 274–299
87. Shibata S, Shibata T, Imamura M, Ohkubo T, Satoh S, Uwamino Y, Nogawa N, Baba M, Matsuyama S, Iwasaki S (1994) Measurement of the excitation function for ^{63}Cu (n, p) ^{63}N. Annual report, Institute for Nuclear Study, University of Tokyo, p 123
88. Straume T (1993) Neutron discrepancies in the dosimetry system 1986 have implications for radiation risk estimates. RERF Update 4: 3–4
89. Straume T (1996) Risk implications of the neutron discrepancy in the Hiroshima DS86 dosimetry system. Radiat Prot Dosim 67: 9–12
90. Knie K, Faestermann T, Korschinek G (1997) AMS at the Munich gas-filled analyzing magnet system GAMS. Nucl Instr Methods Phys Res B 123: 128–131
91. Bormann M, Jeremie H, Andersson-Lindström G, Neuert H, Pollehn H (1960) Über die Wirkungsquerschnitte einiger von 14 MeV-Neutronen in den Szintillationskristallen NaJ(Tl), KJ(Tl), CsJ(Tl) und ^{6}LiJ(Eu) ausgelösten Kernreaktionen. Z Naturforsch [A] 15: 200–210
92. Dixon WR, Aitken JH (1961) Absolute cross section of the ^{39}K(n,p)^{39}Ar reaction for 2.5 MeV neutrons. Nucl Phys 24: 456–464
93. Bass R, Häenni HP, Bonner TW, Gabbard F (1961) Disintegration of ^{39}K by fast neutrons. Nucl Phys 28: 478–493
94. Bass R, Fanger U, Saleh FM (1964) Cross sections for the reactions ^{39}K(n,p)^{39}Ar and ^{39}K(n,α)^{36}Cl. Nucl Phys 56: 569–576
95. Johnson PB, Chapman NG, Callaghan JE (1967) The absolute cross sections of the ^{39}K(n,p)^{39}Ar and ^{39}K(n,α)^{39}Ar reactions for 2.46 MeV neutrons. Nucl Phys A94: 617–624
96. Bartle CM, Johnson PB, Chapman NG (1974) Absolute (n,p) and (n,α) cross sections for ^{39}K and ^{40}Ca between 2.4 and 2.9 MeV. Nucl Phys A220: 395–403
97. Aleksandrov DV, Klochkova LI, Kovrigin BS (1975) Cross section of (n,p) reaction on ^{27}Al, ^{28}Si, ^{31}P, ^{35}Cl, ^{39}K and ^{52}Cr at 14.1 MeV neutron energy. Atomnaya Energija 39: 137–139
98. Foland KA, Borg RJ, Mustafa MG (1987) The production of ^{38}Ar and ^{39}Ar by 14 MeV neutrons on ^{39}K. Nucl Sci Eng 95: 128–134
99. Forster M, Moser H, Ramm K, Hietel B (1989) Investigating the neutron-induced subsurface production of environmental isotopes ^{37}Ar, ^{39}Ar, ^{3}H and ^{36}Cl with neutron irradiation of aquifer material. Chem Geol (Isotope Geosci Sect) 79: 325–332
100. Rühm W (1993) Das Neutronenspektrum der Atombombe von Hiroshima und das Dosimetriesystem DS86. PhD Thesis, Technical University Munich (in German)
101. Feige Y, Oltman BG, Kastner J (1968) Production rates of neutrons in soils due to natural radioactivity. Journal of Geophysical Research 73: 3135–3142
102. Dockhorn B, Neumaier S, Hartmann FJ, Petitjean C, Faestermann H, Korschinek G, Morinaga H, Nolte E (1991) Determination of erosion rates with cosmic ray produced ^{36}Cl. Z Phys A – Hadrons and Nuclei 341: 117–119
103. Evans JM, Stone JOH, Fifield LK, Cresswell RG (1997) Cosmogenic chlorine-36 production in K-feldspar. Nucl Instr Methods Phys Res B 123: 334–340
104. Loeken T, Scherer P, Weber HW, Schultz L (1992) Noble gases in eighteen stone meteorites. Chem Erde 52: 249–259
105. Schultz L, Weber HW (1996) Noble gases and H chondrite meteoroid streams: no confirmation. J Geophys Res 101, no. E9, 21: 177–21,181
106. Loosli HH (1983) A dating method with ^{39}Ar. Earth Planet Sci Lett 63: 51–62
107. Conneely CM, Prestwich WV, Kennett TJ (1986) The thermal neutron capture cross section of ^{9}Be. Nucl Instr Methods Phys Res A248: 416–418
108. Lal D, Nishiizumi K, Reedy RC, Suter M, Wölfli W (1987) An accurate measurement of the ^{10}B(n,p)^{10}Be cross section at thermal energies. Nucl Phys A248: 189–192
109. Synal HA, Bonani G, Döbeli M, Ender RM, Gartenmann P, Kubik PW, Schnabel C, Suter M (1997) Status report of the PSI/ETH AMS facility. Nucl Instr Methods Phys Res B123: 62–68
110. Heisinger B, Niedermayer M, Hartmann FJ, Korschinek G, Nolte E, Morteani G, Neumaier S, Petitjean C, Kubik P, Synal A, Ivy-Ochs S (1997) In-situ production of radionuclides at great depths. Nucl Instr Methods Phys Res B123: 341–346
111. Kawano Y, Ueno Y (1966) K-Ar dating of granites in Japan. V. Granites in southwestern Japan. Ganko 56: 191–211 (in Japanese)
112. Kaizuka S (1969) Transition of geographical features. Kagaku 39: 11–19 (in Japanese)
113. Imai N, Terashima S, Itoh S, Ando A (1995) 1994 compilation values for GSJ reference samples, 'igneous rock series'. Geochem J 29: 91–95
114. Koehler PE, Graff SM (1991) ^{17}O(n,α)^{14}C cross section from 25 meV to approximately 1 MeV. Phys Rev C44: 2788–2793
115. Parker RL (1967) Composition of the earth's crust, data of geochemistry. (Professional Paper 440/D) US Geological Survey
116. Rühm W, Schneck B, Knie K, Korschinek G, Zerle L, Nolte E, Weselka D, Vonach H (1994) A new half-life determination of ^{59}Ni. Planet Space Sci 42: 227–230
117. Pommerance H (1952) Thermal capture cross sections. Phys Rev 88: 412–413
118. Ishaq AFM, Robertson A, Prestwich WV, Kennett TJ (1977) Thermal neutron capture in isotopes of nickel. Z Phys A 281: 365–372
119. Carbonari AW, Peceqvilo BR (1988) Investigation of thermal neutron capture gamma-rays on Ni-58(n,g)Ni-59. Conference Mito, CA09
120. Bergqvist I, Lundberg B (1968) Radiative capture in nickel and bismuth of neutrons in the MeV region. Nucl Phys A120: 161–182
121. Ernst A, Fröhner FH, Kompe D (1970) Proceedings of the International Conference on Nuclear Data for Reactors, Helsinki, Vol 1. IAEA, Vienna, p 633
122. Lindholm A, Nilsson L, Ahmad M, Anwar M (1980) Direct-semidirect and compound contributions to radiative neutron capture cross sections. Nucl Phys A339: 205–218
123. Wisshak K, Käppeler F, Reffo G, Fabbri F (1984) Neutron capture in s-wave resonances of iron-56, nickel-58, and nickel-60. Nucl Sci Eng 86: 168–183
124. Kaiser WA, Berman BL (1972) The average ^{130}Ba(n,γ) cross section and the origin of ^{131}Xe on the moon. Earth Planetary Sci Lett 15: 320–324